Addis Ababa University

Addis Ababa Institute of Technology

School of Civil and Environmental Engineering

School of Civil and Environmental Engineering Postgraduate Program Structural Engineering Stream

USING CARBON FIBER REINFORCING POLYMER TO STRENGTHEN THE FLEXURAL CAPACITY OF DAMAGED POST-TENSIONED BEAMS

by

MARAKI GEDU ANBESSE

Sponsor: FEMALE SCHOLARSHIP/ ALPHA POST-TENSION

September, 2024

A Thesis submitted at Addis Ababa Institute of Technology
in partial fulfillment of the requirements for
the Degree of Master of Science in Structural Engineering

The undersigned have examined the thesis entitled **'USING CARBON FIBER REINFORCING POLYMER TO STRENGTHEN THE FLEXURAL CAPACITY OF DAMAGED POST-TENSIONED BEAMS'** presented by **MARAKI GEDU ANBESSE**, a candidate for the degree of Master of Science and hereby certify that it is worthy of acceptance.

Abrham Gebre (PhD)		Oct. 15/2024.
Advisor	Signature	Date
ESAYAS G/yohannes (PhD)		Oct-14-2024
Internal Examiner	Signature	Date
Edom Adane (Ph.D)		Oct-16-2024
External Examiner	Signature	Date
Chair Person	Signature	Date

Abrham Gebre (Dr.)
Dean, School of Civil & Environmental Engineering

UNDERTAKING

I certify that the research work titled "**USING CARBON FIBER REINFORCING POLYMER TO STRENGTHEN THE FLEXURAL CAPACITY OF DAMAGED POST-TENSIONED BEAMS**" is my own work. The work has not been presented elsewhere for assessment. Where material has been used from other sources, it has been properly acknowledged /referred.

Maraki Gedu

Abstract

Post-tensioning is a type of pre-stressing in which high-strength steel strands or bars; commonly referred to as tendons, are used to reinforce (strengthen) concrete or other materials. Carbon fiber-reinforced polymers on the other hand are incredibly light and strong fiber-reinforced plastics that are used to enhance concrete structures by bonding the polymer to the concrete member.

Damage to structural members can occur due to different reasons in various real-world applications. Similarly, post-tensioned members can also be subjected to damage due to various reasons, such as accidental cutting or drilling into tendons, failures in anchorage and dead end zones resulting from issues like insufficient anti-burst reinforcement, misalignment of the anchor, and improper material utilization. These problems can lead to the loss of prestressing force in post-tension strands, which in turn can decrease the load carrying capacity of the elements, particularly their flexural capacity. This thesis paper investigates the potential of Carbon Fiber-Reinforced Polymer (CFRP) strengthening in enhancing the flexural capacity of damaged post-tensioned concrete beams.

Employing an experimental program, the study compares the performance of control beams to beams strengthened with varying CFRP layers. Results demonstrate a significant increase in flexural capacity, averaging 41.5% per CFRP layer, highlighting the effectiveness of this strengthening technique. How varying amount of post tensioning and CFRP wraps affect cracks and delamination patterns of carbon fiber were also studied and discussed in detail. Further exploration into alternative fiber types and testing configurations is recommended. .

Keywords: Post-tension, Post-Tensioned Beams, FRP, CFRP

ACKNOWLEDGMENTS

First and foremost I would like to thank our Almighty God for he gave me success in my efforts. Then my greatest gratitude goes to my Sponsor Alpha Post tension PLc who did not just provide all the materials but was with me for all the ups and downs of this journey. I am without words to express my heartfelt appreciation for all the workers of Alpha Post Tension PLc, Specially our General Manager Abel Gebresadik and our Design Manager Ephrem Beyene, who put their time & energy into this project from the inception of this research through its completion.

My acknowledgment also goes to my advisor Dr. Abrham Gebre (Phd) for his consistent support throughout this thesis project and for his timely feedback's and suggestions which made all the difference. And finally, I would like to mention my family and my lovely husband, who has always shared my challenges, good and bad times, and made the journey a memorable one.

Contents

1 Introduction **1**

1.1 Background 2

1.1.1 Post Tension 2

1.1.1.1 Damages to Post Tension Members 2

1.1.2 CFRP 3

1.2 Statement of Problem 4

1.2.1 General Objective 4

1.2.2 Specific Objectives 4

1.3 Scope 4

1.4 Significance of the Research 5

2 Literature Review **6**

2.1 Historical Development of Post Tensioned Concrete 6

2.2 Basic Concept of Pre-stressing 7

2.3 Problems Faced by the Post-Tensioning Industry 8

2.4 Introduction to FRP (Fiber Reinforcing Polymer) 9

2.5 Historical Overview of FRP 10

2.6 Basic Concepts of FRP 11

2.6.1 Types of FRP, Selection and Applications 11

2.6.2 Properties of Structural Adhesives 13

2.7 Strengthening of Structural Members 13

3 Experimental Program **15**

3.1 Material Properties 15

3.1.1 Concrete 15

3.1.1.1 Cement 15

3.1.1.2 Fine and Coarse Aggregates 16

3.1.2 Post Tensioning (Tendons) 16

3.1.3 CFRP Material 17

3.1.4 Reinforcement bar 18

3.2 Test Specimens 18

3.2.1 The Fabrication of Test Beams 19
3.3 Experimental Setup 22
3.3.1 Instrumentation & Data Acquisition 22

4 Results and Discussion **23**
4.1 Beam Series - 1 23
4.2 Beam Series - 2 25
4.3 Capacity Analysis According to ACI 28
4.4 Compression Limit Analysis 29

5 Conclusion and Recommendation **31**
5.1 Conclusions 31
5.2 Recommendations 33

A Appendices **38**
A.1 Section Analysis of Control Beams G2B-20 and G3B-20 38
A.2 Section Analysis of CFRP Wrapped Test Beams (G2B-11 and G3B-22) . 41
A.3 Detailed Material Test Results From the Experimental Program 45
A.4 Detailed Experiment Results 47
A.4.1 Beam Series - 1 47
A.4.1.1 Beam Series 1 - Control Beam 1 (G2B-20) 47
A.4.1.2 Beam Series 1 - Control Beam Two (G2B-10) 48
A.4.1.3 Beam Series 1 - Test Beam One (G2B-11) 50
A.4.1.4 Beam Series 1 - Test Beam Two (G2B-12) 52
A.4.2 Beam Series - 2 54
A.4.2.1 Beam Series 2 - Control Beam One (G3B-30) 54
A.4.2.2 Beam Series 2 - Control Beam Two (G3B-20) 56
A.4.2.3 Beam Series 2 - Test Beam One (G3B-21) 57
A.4.2.4 Beam Series 2 - Test Beam Two (G3B-22) 59

List of Tables

3.1 Mix Design of Concrete 16
3.2 Designation of Beam Specimens 20

4.1 Result Summary of the Experimental Program 29
4.2 Compressive Forces of Experimental Beams 30

A.1 Sieve Analysis of Natural Sand 45
A.2 Sieve Analysis of Crushed Sand 45
A.3 Particle Size Analysis of Gravel (9.5mm - 25mm) 46
A.4 Particle Size Analysis of Gravel (4.75mm - 9.5mm) 46
A.5 G2B-20 Crack Summary 47
A.6 G2B-20 Crack Summary After Unloading 47
A.7 G2B-10 Crack Summary 49
A.8 Crack Width After Unloading of Beam G2B-10 49
A.9 G3B-30 Crack Summary 54
A.10 G3B-30 Right Side Crack Summary After Unloading 54
A.11 G3B-30 Left Side Crack Summary 55
A.12 G3B-20 Crack Summary 56
A.13 G3B-20 Left Side Crack Summary After Unloading 56

List of Figures

1.1 Instance of Anchorage Zone Failure 3

2.1 Post Tensioned Beam with Bonded Tendons 7
2.2 Most Commonly Used CFRP Types and Accessories 12

3.1 Post tensioning Wedge and Anchor Block 17
3.2 Grouting Machine, Grouting Tube 17
3.3 CFRP Sheet Used 17
3.4 Test Beams Cross-Section 19
3.5 Onion Form of Dead Ends of Strands 19
3.6 Polishing & Primer Application (left to right) 21
3.7 Wrapping of CFRP 21
3.8 Testing Machine Setup 22
3.9 Experimental setup with one point loading 22

4.1 Failure of G2B-20 24
4.2 Load-deflection curves of control and strengthened beams (Group-1) . . . 24
4.3 a) deformed shape of G2B-11 and b) rupture and delamination of CFRP, G2B-12 25
4.4 Flexural failure of G3B-30 25
4.5 Load deflection diagram of G3B beam series 26
4.6 Rupture and delamination of a) G3B-21 and b) G3B-22 27
4.7 Rupture and delamination of a) G3B-21 and b) G3B-22 28

A.1 Filtered Load Vs Deflection of G2B-20 48
A.2 Close up on the Failure State of G2B-20 48
A.3 Filtered Load Vs Deflection of G2B-10 49
A.4 G2B-10 After Failure 50
A.5 Filtered Load Vs Deflection of G2B-11 50
A.6 Concrete Crushing and Spalling at top of the beam 51
A.7 G2B-11 After Testing Bottom, Right & Left Side CFRP Tear & Delamination (right, left & bottom) 51

A.8 Filtered Load Vs Deflection of G2B-12 52
A.9 Concrete Crushing and Spalling at top of the beam 52
A.10 G2B-12 Right Side CFRP Tear & Delamination 53
A.11 G2B-12 Left Side CFRP Tear & Delamination 53
A.12 Spalled Concrete Beneath the Beam G2B-12 53
A.13 Right Side Failure State of G3B-30 54
A.14 Filtered Load Vs Deflection of G3B-30 55
A.15 G3B-30 Flexural Crack and Concrete Crushing at Mid Span & at Support 55
A.16 Filtered Load Vs Deflection of G3B-20 56
A.17 G3B-20 Flexural Crack and Concrete Crushing (Top & Bottom Center) . 57
A.18 Filtered Load Vs Deflection of G3B-21 57
A.19 G3B-21 After Failure 58
A.20 G3B-21 Right Side Tear & Delamination 58
A.21 G3B-21 Left Side Tear & Delamination 58
A.22 Load Vs Deflection of G3B-22 59
A.23 Concrete Crushing and Spalling at Bottom of the Beam G3B-22 59
A.24 G3B-22 Right Side Tear & Delamination 60
A.25 G3B-22 Left Side Tear & Delamination 60

List of Symbols

$f_c^{'}$	Concrete Compressive Strength
α_L	Coefficient of Thermal Expansion
T_g	Glass Transition Temperature
^0C	Degree Celsius
f_{pu}	Post Tension Strand Ultimate Strength
f_{ps}	Stress in the prestressed reinforcement
f_y	Reinforcing Rebar Yield Strength
A_{st}	Area of Tension Steel
A_{sc}	Area of Compression Steel
A_{pt}	Area of Post Tension Steel
A_f	Cross-sectional Area
b	Width of beam
d	Depth of Beam
L	Length of the Beam
$d^{'}$	Effective Depth of beam
d_p	Depth of Post Tensioning Strand
$d_c^{'}$	Depth of the Compression Steel
γ_p	Factor for the influence of different types of prestressing reinforcement
β_1	Factor for relaxation of prestressing steel
ρ_p	Increased value of f_{ps} due to the prestressed steel
ρ	Increased value of f_{ps} obtained when tension reinforcement is provided
$\rho_{\prime}$	Increased value of f_{ps} obtained when compression reinforcement is provided
$C_s^{'}$	Force of the Compression Steel
T_{ps}	Force of the post tensioning steel
T_s	Force of the Tension Steel
T_{cf}	Force of the CFRP
a	Depth of the compression zone
c	Neutral Axis Depth
$\xi_{\mathrm{s}}^{\prime}$	Strain in the Compression steel
ξ_{s}	Strain in the Tension steel
$\xi_{\mathrm{s,pt}}$	Strain in the Post Tension Steel
$\xi_{\mathrm{s,cf}}$	Strain in the CFRP
W_u	Beam self Weight
M_u	Ultimate Moment Capacity of the beam
P_u	Point Load Capacity of the beam
δ	Compressive Stress

F	Force
A	Area
M	Bending Moment
y	Maximum Distance from Neutral Axis
I	Moment of Inertia
f_l	Maximum Confinement Pressure
E_f	CFRP Modulus of Elasticity
n	Number of Layers of CFRP applied
t_f	Thickness of CFRP wrap
ε_{fe}	Effective Strain in the CFRP at failure
D	Effective width of CFRP Confining action in Non-Circular Elements
F_c	Force of Confinement

List of Abbreviations

ACI	American Concrete Institute
AFRP	Aramid Fiber Reinforcing Polymer
ASCE	American Society of Civil Engineers
ASTM	American Society for Testing and Materials
CDE	Construction Durability Engineers
CFRP	Carbon Fiber Reinforcing Polymer
CFRTP	Carbon-Fiber Reinforced Thermoplastic
CRP	Carbon-Fiber-Reinforced Plastics
E	Modulus of Elasticity
EB-CFRP	Externally Bonded - Carbon Fiber Reinforcing Polymer
FRC	Fiber Reinforced Concrete
FRP	Fiber Reinforcing Polymer
FRP EBR	Fiber Reinforcing Polymer - Externally Bonded Reinforcing
GPa	Giga Pascal
GFRP	Glass Fiber Reinforced Polymer
HM	High Modulus
Kg	Kilogram
kN	Kilo Newton
LVDT	Linear Variable Displacement Transducer
MPa	Mega Pascal
NSM-CFRP	Near-Surface Mounted Carbon-Fiber-Reinforced Polymer
OPC	Ordinary Portland Cement
PC	Post Tension Concrete
P-SWR	Prestressed Steel Wire Ropes
PT	Post Tension
PTI	Post Tension Institute
RC	Reinforced Concrete
SFRC	Steel Fiber Reinforced Concrete
TOCIEJ	The Open Civil Engineering Journal

Chapter 1

Introduction

Damage to concrete structures can occur in various ways throughout their service life. These damages can be classified in different ways, such as by type, cause, attack mechanism, frequency of defects, financial loss due to defects, and extent of repair measures[1]. When dealing with post-tensioned members, additional specific problems may arise. These structures may suffer damage from strand corrosion, accidental impact, brittle wire cracking, coring or drilling after construction, as well as failures in anchorage and dead end zones resulting from insufficient anti-burst reinforcement, anchor misalignment, and improper material utilization. These issues ultimately lead to tendon failures[1]. Tendon failures mainly result in the loss of the initially applied pre-stressing force that was applied to them.

Pre-stressing loss in prestressed concrete elements is a phenomenon that occurs when the actual prestress force decreases due to various factors. In addition to physical damages to the post-tension tendons mentioned above, several other factors also contribute to prestressing loss. These factors include prestressing tendon relaxation, frictional losses, and elastic shortening of concrete, among others.

To mitigate these losses and ensure the desired level of force remains effective in prestressed concrete members, engineers often account the losses during the design process by considering appropriate allowances and adjustments in prestress force estimates[2]. Additionally, implementing robust quality control measures during construction, such as employing appropriate tendon tensioning techniques and diligent monitoring, can effectively mitigate prestress losses and uphold the structural integrity of prestressed concrete elements[3]. In situations where these losses reach a critical level, it becomes imperative to strengthen the member using various strengthening techniques. One common technological advancement that can be utilized is the application of Carbon Fiber Reinforced Polymer (CFRP) to enhance the load-carrying capacity, durability, and service life of the structure[4, 6, 5].

1.1 Background

1.1.1 Post Tension

Concrete is known as one of the best materials to bear the compressive loading, however when it comes to tensile strength, unfortunately, it does not stand anywhere. That's why reinforcement in the form of steel wires is used in concrete beams, slabs and many other units to bear the tensile loading. And the unique concept of Pre-stressing of concrete that dates back to 19th century, counterbalances the external tensile stress by advanced compression.

Post-tensioning specifically is one form of pre-stressing in which reinforcing (strengthening) of concrete or other materials is done with high-strength steel **strands** or bars, typically referred to as **tendons**. Post-tensioning tendons, which are pre-stressing steel cables inside plastic ducts or sleeves, are positioned in the forms before the concrete is placed. Afterwards, once the concrete has gained strength but before the service loads are applied, the cables are pulled tight, or tensioned, and anchored against the outer edges of the concrete[7].

Common Applications for PT Post-tensioning, also known as PT, has gained significant popularity in various countries over the last three decades due to advancements in technology. While there were once concerns regarding cable corrosion, particularly in parking structures exposed to deicing salt, these issues have largely been resolved through the use of superior materials, improved construction techniques, and comprehensive training and certification programs[7]. However, it is worth noting that post-tensioning has yet to gain widespread recognition and acceptance in our country, Ethiopia.

1.1.1.1 Damages to Post Tension Members

Post-tensioned structures are susceptible to various factors that can result in tendon failure. Firstly, the presence of moisture over time can cause corrosion and eventual rupture of the tendons. Secondly, when coring, drilling, or cutting through an already constructed post-tensioned member, there is a risk of inadvertently severing a tendon, thereby releasing the compressive force applied to the member. If the structure is not grouted, this can lead to serious issues due to the potentially explosive release of tensile force. While grouted structures reduce the risk, the tendon still experiences a loss of its pre-stressing force. Additionally, failures in the anchorage zone can also damage post-tensioned members. These failures can occur due to several reasons, including insufficient anti-burst reinforcement, anchor misalignment, and improper material utilization, among others[11].

All of these issues typically lead to the loss of pre-stressing force in the post tension

Figure 1.1: Instance of Anchorage Zone Failure

tendons. When strands are drilled or cut, resulting in complete severing of strands, the tendons will lose 100% of their pre-stressing force. On the other hand, problems such as anchorage zone failures, as shown in figure 1.1, could cause the tendons to loosen and result in a lesser percentage loss of pre-stressing force.

1.1.2 CFRP

Carbon-Fiber-Reinforced Polymers (CFRPs), Carbon-Fiber-Reinforced Plastics, and Carbon-Fiber Reinforced Thermoplastic (CFRP, CRP, CFRTP), also referred to as carbon fiber, carbon composite, or simply carbon, are fiber-reinforced plastics that possess exceptional strength and lightness. These materials incorporate carbon fibers and are widely utilized in applications where a high strength-to-weight ratio and stiffness (rigidity) are crucial, such as aerospace, ship superstructures, automotive, and sports equipment[8]. One of the most recent advancements in the use of CFRPs is their application in the reinforcement of structural elements, which serves as the primary focus of this paper.
Limited research has been produced on strengthening Prestressed concrete members. Parallel with the scarcity of in situ installations, as reported by FIB Task Group 9.3, less than 10% of FRP (Fiber Reinforcing Polymer) strengthened bridges as of 2001 are pre-stressed][8]. Strengthening usually takes place when all long-term phenomena (creep, shrinkage, relaxation) have fully developed, which may complicate the preliminary assessment of the existing conditions. Apart from this, the conventional verification procedures adopted for Pre-stressed members can be applied, provided that the FRP contribution is appropriately considered. As in RC (Reinforced Concrete) strengthening, the required amount of FRP will generally be governed by the ultimate limit state design in the members. However, additional failure modes controlled by rupture of the pre-stressing tendons must also be considered, and consideration should be given to limitations on cracking. In the latter case, the possibility of admitting tensile stresses in the PT (Post Tension) section after FRP strengthening is the subject of ongoing debate[8, 9].

1.2 Statement of Problem

Damage to post-tensioned members can arise from various factors, including tendon corrosion, accidental damage such as cutting or drilling into tendons after construction, and failures in the anchorage and dead end zones. This study addresses the post-tensioning issues related to the loss of prestressing force in these members due to the aforementioned damages. It focuses on investigating how post-tensioned beams with these issues can be strengthened using Carbon Fiber Reinforced Polymer (CFRP) and the extent to which their load-carrying capacity can be enhanced through this strengthening technique.

1.2.1 General Objective

- ▷ To investigate the performance of carbon fiber reinforced polymer (CFRP) strengthened post-tensioned beams with damage and assess the application techniques that enhance their performance. The study aims to analyze the increase in stress-carrying capacity of these damaged beams and examine the interaction between post-tensioning and CFRP.

1.2.2 Specific Objectives

- ▷ To present the correlation between the increase in load capacity of the PT (Post Tension) beam with the number of wraps of CFRP.
- ▷ To study the failure modes of CFRP wrapped post tensioned beams.
- ▷ Aims to analyze the impact of post-tensioning on the closing or receding of cracks in members during the unloading process.

1.3 Scope

This study explores the potential of CFRP strengthening techniques in enhancing the flexural capacity of post-tensioned concrete beams with pre-stressing loss (specifically at 50% and 66.7% prestress levels). Through an experimental program, the study compares the performance of control beams with those reinforced using varying layers of CFRP. Additionally, the research analyzes the impact of different prestressing levels and CFRP wraps on the formation of cracks and delamination patterns in carbon fiber. It should be noted that this study will not cover deep beams, short beams, beam-columns, or beams made of high-strength concrete. Furthermore, the focus of this study is solely on the enhancement of flexural strength in PT beams, with no consideration given to shear strengthening.

1.4 Significance of the Research

This study has a significant impact on the strengthening industry of Ethiopia. It allows for a better understanding of the CFRP technique of strengthening, enabling its efficient utilization. Given that both post-tensioning and CFRP strengthening are relatively new technologies in our country, this study contributes to facilitating the adoption of these technologies in our construction industry.

1.5 Organization of the Thesis

Chapter 1 provides an introductory overview of the key concepts discussed in the paper, as well as an explanation of the research objectives and scope.
Chapter 2 offers a historical development of both post-tensioning and CFRP strengthening methods. It explores their applications and provides a comprehensive literature review of relevant papers.
Chapter 3 describes the experimental program, including the methodology employed and a detailed explanation of the methods and procedures used. This section also outlines the instrumentation utilized, as well as the analysis and tests conducted on the appropriate specimens. It further discusses the material properties, specimen fabrication, and test setup.
Chapter 4 presents the experimental results, discussing them individually and in conjunction with relevant data from other researchers.
Chapter 5 concludes the study by presenting observed facts and phenomena, along with recommendations for future studies and areas that were not explored due to limitations.
The Appendix section A.1 and A.2 provide a detailed analysis of the CFRP unwrapped and wrapped beams, respectively. Appendix A.3 presents comprehensive material test results from the experimental program. Lastly, appendix A.4 presents the detailed experiment results of the test beams.

Chapter 2

Literature Review

This chapter presents the findings from different reviewed literature on the subject of Post tensioning, post-tensioned beams, FRP strengthening and retrofitting works.

2.1 Historical Development of Post Tensioned Concrete

Pre-stressed concrete is not a novel idea; in 1872, Californian engineer P.H. Jackson received a patent for a pre-stressing method that involved building beams or arches out of individual blocks using a tie rod. German inventor C.W. Doehring received a patent in 1888 for using metal wires to pre-stress slabs. However, because the pre stress eventually fades, these early attempts at pre-stressing were not very effective[10]. After a long lapse of time during which little progress was made because of the unavailability of high-strength steel to overcome pre-stress losses, R.E. Dill of Alexandria, Nebraska, recognized the effect of the shrinkage and creep (transverse material flow) of concrete on the loss of pre stress. Later, he devised the concept that the time-dependent loss of stress in the rods caused by the member's shrinkage and creep would be compensated for by consecutive post-tensioning of unbonded rods[10].

In the early 1970s the market for post-tensioning in buildings was rapidly growing. More engineers were learning how to design post-tensioned buildings and, as a result, more post-tensioned buildings were being built worldwide. And one of the main reasons for this development was the advancement in computers which could efficiently handle PT design calculations[11].

Today, pre-stressed concrete is used in buildings, underground structures, TV towers, floating storage and offshore structures, power stations, nuclear reactor vessels, and numerous types of bridge systems including segmental and cable-stayed bridges. The success in developing and constructing landmark structures worldwide has been greatly attributed to advancements in material technology, specifically pre-stressing steel, and the accumulated knowledge in estimating short- and long-term losses in pre-stressing forces[10].

2.2 Basic Concept of Pre-stressing

Pre-stressing is a way of counteracting the effect of external loads on a structure by imposing a state of stresses contrary to the load effects. The most common way to achieve this is by means of tendons, which are stressed prior to final loading of the structure[11]. Pre-stressed concrete is a comprehensive term encompassing both pre-tensioned and post-tensioned concrete. The terms "pre" and "post" refer to the timing of stress application to the pre-stressing tendons in relation to the placement and curing of the concrete[11]. In pre-tensioned concrete, the tendons are usually positioned in steel bed forms and stressed before the concrete is poured. The pre-stressing steel is generally straight or "harped" in straight segments, referred to as "**Profiles**" and is a critical factor influencing the influence of the strands on the structural elements[11]. In the majority of post-tensioned members in real-life applications, the tendons are commonly arranged in a parabolic profile within the concrete forms and subsequently stressed after the casting process.
Another classification is bonded and unbonded post-tensioning. Unbonded post-tensioning typically involves single (mono) strands or threaded bars that remain unbonded to the surrounding concrete, allowing them the flexibility to move locally in relation to the structural member[12]. For bonded systems, the prestressing steel is encased in a corrugated metal or plastic duct. Once the tendon is stressed, cementitious grout is injected into the duct to ensure its bonding with the surrounding concrete[7]. Figure 2.1 below shows an example of on site installations of a bonded PT beam before and after casting, which is the main focus of this paper.

Figure 2.1: Post Tensioned Beam with Bonded Tendons

2.3 Problems Faced by the Post-Tensioning Industry

As discussed earlier, there are several unique challenges associated with post-tensioned members. These challenges include the corrosion of tendons, damage to post-tension strands (such as drilling or cutting), stress reversals, restraint to concrete volume change (shortening), and failures in the anchorage zones.

The primary cause of post-tensioning tendon corrosion is the presence of moisture. Over time, moisture can weaken the tendons, eventually leading to their failure. Moisture can enter the PT system through various pathways, including entering the sheathing before or during construction (such as when strands are left unprotected at the plant, during shipping, or at a construction site), penetrating cracks and joints, and reaching unprotected portions (un-grouted) of the PT system during the building's service life, among other ways[16]. In the early stages, it became evident that the unbonded tendon sheathings and coatings (grease) used at that time were insufficient for aggressive environments, particularly those where de-icing salts are regularly applied to exposed concrete surfaces. Within approximately 10 years of service, significant corrosion issues started to arise in buildings subjected to such conditions[11].

Restraint to concrete volume change (shortening) is a significant and pervasive challenge faced by the industry, especially during the early stages of the technology development. The mechanics of volume change and the corresponding restraint differ between post-tensioned concrete members and non-prestressed members. The axial pre-stress force effectively mitigates the formation of cracks that would otherwise occur due to shortening between the ends of the member. However, unlike non-prestressed members, post-tensioned concrete members experience significant inward movement at the ends in response to total volume change along the length. As a result, substantial shears and moments are induced in the connected walls and columns, which can lead to the development of unsightly and sizable cracks in both the post-tensioned member and the associated walls and columns[11].

In post-tensioning, the required depth is smaller, resulting in a reduced cross section. This reduction in size, especially for PT beams and PT slabs, can restrict the use of anchorage devices in the anchorage zone. Analytical modeling and assessment have demonstrated that the limited use of anchorage devices can lead to anchorage failure, thereby reducing the capacity of the members[13]. Another literature also demonstrates that bursting of the end anchorage leads to reduced capacity and uncontrolled collapse of the PT structure. Moreover, lack of proper anchorage detail leads to a significant reduction in the ultimate strength of beams[13].

During the post-tensioning process, the failure of the end anchorage has been found to be critical, with test findings revealing the presence of concentrated cracks near the anchorage zone[14]. Several other studies have also been conducted to investigate techniques

for enhancing the performance of the anchorage zone in post-tensioned members. In line with this, in one study a steel fiber reinforced concrete (SFRC) was utilized near the anchorage zone to improve its performance and reduce the amount of steel required in a post-tensioned bridge in Florida. The results indicated that the addition of 1.5% steel fiber enhanced the strength by up to 22% and improved the performance of the anchorage zone[15].

2.4 Introduction to FRP (Fiber Reinforcing Polymer)

FRP is a composite material comprising a polymer matrix reinforced with fibers in the form of fabric, mat, or strands. It was first used in Japan in the 1980s but mainly developed in Switzerland. FRP can be applied in beams, slabs, and columns to improve flexural, shear, and compressive strength (confinement)[17]. Its application range include

- ▷ Load Increase - Increase carrying capacity in buildings, bridges, allows for installation of heavy equipment in industrial facilities, increase vibration in structures and etc...
- ▷ Improve Structural Condition - Reduce deformations, reduce stresses in existing structural elements, limit or arrest crack propagation...[18]
- ▷ Seismic Retrofitting - Columns wrapping reinforcement for improving ductility and shear strength, masonry walls reinforcement for improving out-of-plane bending and in-plane shear strengths, beam and slab reinforcement...
- ▷ Aging and Damaged Structures - Aging of old deteriorated construction materials, corrosion of steel bars in concrete, vehicles collusion impact on structures (impact damage)
- ▷ Design or Construction Errors - Lack of adequate well-detailed reinforcing bars, inadequate member cross section, substandard concrete material strength[18]

Fiber reinforced plastic (FRP) reinforcement is crucial for strengthening and rehabilitating reinforced concrete (RC) structural elements as an external reinforcement. There have been significant advancements in materials, methods, and techniques for structural strengthening. The use of carbon fiber reinforced polymer (CFRP) offers numerous advantages due to its excellent properties, including:

- ▷ Non corrosive, High temperature resistance, limited creep resistance under high permanent loads, and excellent seismic strengthening system.
- ▷ Very high strength, high modulus, high durability, high fatigue resistance (allows for long operation projects and extended deadlines), high alkali resistance (anti-acid, alkali and other chemical corrosion and resistance to severe environments).

- ▷ Lightweight (adds almost no additional weight to the existing structure), Low overall thickness, easy to transport (rolls)[17, 18].
- ▷ The application of this product is unlimited in length and has a wide range of uses. It is suitable for various structural components such as beams, columns, ventilation tubes, pipes, and walls. It can be used on different types of structural components and systems, including concrete structures, masonry structures, wood structures, steel structures, and many other elements and systems.
- ▷ CFRP materials have Linear Stress-strain relationship up to breakage[17, 18]

Although small Carbon fiber also has some disadvantages which include;

- ▷ Carbon fiber is conductive, safety measures should be taken to prevent electric shocks.
- ▷ Carbon fiber sheets should not be bent during transportation, handling, and cutting process which make them somewhat difficult to handle.
- ▷ During transportation and storage, carbon fiber materials shall not be squeezed or compressed, so as to avoid carbon fiber damage, and shall not be exposed to direct sunlight and/or rain.[18]

2.5 Historical Overview of FRP

FRP, a technology that was started in the 1970s, is relatively early in its development. In Europe, FRP systems were created as substitutes for steel plate bonding. The technique of bonding steel plates to the tension zones of concrete members using adhesive resins has been proven effective in increasing their flexural strengths. This method has been widely used to reinforce bridges and buildings globally. Researchers have explored FRP materials as an alternative to steel because steel plates can corrode, leading to a deterioration of the bond between the steel and concrete. Additionally, steel plates are difficult to install and require the use of heavy equipment[19].
Experimental work on using FRP materials for strengthening concrete structures was first reported in Germany in 1978 by Wolf and Miessler (1989). The research conducted in Switzerland paved the way for the first applications of externally bonded FRP systems in flexural strengthening of reinforced concrete bridges (Meier, 1987; Rostasy, 1987). In the 1980s, Japan applied FRP systems to reinforced concrete columns to enhance confinement, as initially proposed by Katsumata (1987)[19].

2.6 Basic Concepts of FRP

Reinforced and pre-stressed concrete structures are prone to significant degradation in strength and serviceability. However, thanks to advancements in strengthening and retrofitting techniques such as CFRP, concrete structures continue to be widely used in construction. One widely adopted solution for strengthening existing flexural members is the application of external FRP laminates, which provide additional tensile reinforcement[8]. The mechanical properties of composites depend on several factors, including the properties of the fibers, matrix, fiber-matrix bond, and the amount and orientation of the fibers. However, the fibers play a dominant role in bearing the stress in the composite. Thermoset resins like epoxy are commonly used as binding polymers to attach the CFRP to the members, although other thermoset or thermoplastic polymers like polyester, vinyl ester, or nylon are sometimes used. The properties of the final CFRP product can be influenced by the type of additives introduced to the binding matrix (resin). Silica is the most common additive, but rubber and carbon nanotubes can also be used as additives. Carbon Fiber Reinforced Polymer (CFRP) has been proved to enhance the flexural strength of Reinforced Concrete (RC) columns and there is a wide range of its application all over the world but almost no research has been done on strengthening of PT (Post tensioned) beams with CFRP[8].
FRPs are brittle materials due to the fibers exhibiting linear elastic behavior until failure. Therefore, in elements that are externally strengthened with FRP laminates, in addition to concrete crushing or steel reinforcement rupture, the external reinforcement might experience a crisis due to FRP debonding at the ultimate condition. Concrete or steel failure occurs with varying degrees of ductility in the element, whereas delamination occurs in a highly brittle manner. Delamination is a mechanism that relies on the bond along the interfacial surface and typically leads to concrete peeling, as the tensile strength of concrete is significantly lower than that of the adhesive[8].

2.6.1 Types of FRP, Selection and Applications

Based on Fiber type

1. Glass Fiber Reinforced Polymer (GFRP)

- ▷ Density: 1.2 – 2.1 g/cm3
- ▷ α_L = 6 to 10 x10^{-6} ºc
- ▷ T_g= 275^{o}c [17]

2. Carbon Fiber Reinforced Polymer (CFRP)

▷ Density: 1.5 – 1.6 g/cm3

▷ α_L = -1 to 10 x10^{-6} ^{o}c

▷ T_g= 1000^{o}c [17]

3. Aramid Fiber Reinforced Polymer (AFRP)

▷ Density: 1.2 – 1.5 g/cm3

▷ α_L = -6 to -2x10^{-6} ^{o}c

▷ T_g= 1000^{o}c [17]

CFRP is less affected by environmental conditions, has better creep and fatigue resistance as well. CFRP with fiber content of >68% is the most commonly used material around the world[17]. CFRP is available in various forms, including plates, rods, and wraps; which will be specifically addressed in this paper. Figure 2.2 provided below illustrates the aforementioned types. Additionally, it is worth noting that pre-stressed FRP can also be utilized, where the fibers used are pre-stressed.

Figure 2.2: Most Commonly Used CFRP Types and Accessories

Strengthening with FRP is a viable solution for various scenarios, including increasing the capacity of slabs, beams, and bridges. It proves useful when there is a need to accommodate changes in building use or when structural elements have been damaged. Additionally, FRP strengthening can lead to improvements in serviceability, such as reducing deflection and crack width, as well as reducing stress in steel reinforcement. It is also applicable when changes are made to the structural system or when there are modifications in specifications due to earthquakes or changes in design philosophy. Furthermore, FRP strengthening can effectively address design or construction defects, such as inadequate reinforcement or insufficient depth[17].

2.6.2 Properties of Structural Adhesives

Depending on the method of CFRP strengthening technique employed, different types of adhesives can be used. If manual lay-up is used, the adhesive is also the resin for the composite fibers, and if pre-formed FRP composites are used the composite has to be attached to the structural element using a separate adhesive.
To obtain a good performance of concrete structures strengthened with externally bonded FRP reinforcement, adhesives should meet certain requirements[19]. Although detailed studies on the influence of material properties of adhesives on the performance of FRP are rather limited, the following is generally required:

- ▷ Working characteristics with respect to mixing, application and curing should allow excellent joint quality, adequate adhesion to the concrete and the FRP (wetting ability), gap-filling properties, work-ability on overhead surfaces, etc. The adhesive should also be able to attach FRP without the need for temporary fixings[19].
- ▷ Bond quality and work-ability should not be unduly sensitive to limited variations in the quality of the prepared surfaces or the environmental conditions.
- ▷ With respect to durability, the adhesive should exhibit good moisture resistance, low creep, thermal stability and resistance to the alkaline nature of the concrete.
- ▷ The glass transition temperature of the adhesive should be significantly higher than the service temperature.
- ▷ The flexural modulus (E-modulus in bending) should fall within a specified range, generally taken as 2000 to 15000 N/mm2. The lower limit relates to a restriction of creep[19].

2.7 Strengthening of Structural Members

Among the most widely recognized methods for strengthening reinforced concrete structures, the application of externally bonded Fiber Reinforced Polymer (FRP) sheets has gained significant popularity in recent years. This method has been proven to be highly effective in renovating and restoring damaged structures, including buildings and bridges[4]. CFRP, as mentioned above, is an effective strengthening technology due to its high tensile strength, which significantly enhances the performance of structural members. Previous studies have demonstrated that the utilization of a single and two layers of CFRP can increase the ultimate capacity of a beam by at least 18-25% and 40-50%, respectively[6, 20, 21, 22]. Other studies showed that these ranges are applicable to low-strength concrete beams under cyclic loads[24, 23]. A 73% increase was also observed

when old PT girders were strengthened using various FRP methods[5]. The strengthening of PT bridge was also found to be both feasible and cost-effective, resulting in a 50% increase in flexural capacity[25].

A study was conducted to test real-size and small-scale specimens of rectangular and T-section RC beams that were reinforced with CFRP plates. The specimens were subjected to different prestress levels of 0%, 20%, and 40%. The study revealed a significant decrease in the load deflection diagram and observed debonding of the CFRP plates in the large-scale specimens[26]. Furthermore, experimental results demonstrated that using CFRP tendons of different diameters and prestressing levels resulted in significant improvements. Specifically, at a prestress level of 50%, there was a 54% increase in the ultimate load and a 100% increase in the first cracking load[27].

Another study conducted on prestressed concrete beams strengthened with prestressed CFRP sheets demonstrated that the prestressed CFRP sheets efficiently redistributed the applied stresses in the strengthened beam, leading to reduced localized damage. The crack width progression in all tested beams exhibited a linear increase with continuously growing rates during the service state. However, significant increases in cracks were observed beyond the service load levels[28].

When looking at the different types of FRP; a report on unidirectional woven type Glass Fiber Reinforced Polymer (GFRP) showed a 9.8% increase in the flexural capacity of an RC beam[29]. In both experimental and analytical studies conducted on GFRP composites, it was observed that the inclusion of fibers significantly enhances the ultimate load capacity. Specifically, when the fiber is attached solely at the beam's soffit, the load capacity improves by 33%. Furthermore, when U-shaped wrapping is applied up to the neutral axis of the beam, the load capacity shows an even greater improvement of 43%[4].

In this study, the experimental investigation focuses on the utilization of CFRP composites as a flexural enhancing material. The findings demonstrate that the implementation of CFRP leads to a significant improvement in the flexural strength of damaged prestressed concrete beams, achieved through an increase in tensile strength and enhanced overall structural performance.

Chapter 3

Experimental Program

The experimental program of this thesis involves the preparation and testing of concrete beams with different post-tensioning strands and CFRP wraps. The beams have dimensions of 200mm in width, 200mm in depth, and 2m in length. A point loading test is conducted on the beams until they reach their ultimate failure. Additionally, concrete cubes (150mm x 150mm x 150mm) were tested on the 9th, 15th, 27th, and 30th days after casting to determine the concrete strength of the mix used. All experiments were conducted at the Construction Materials Laboratory of Addis Ababa Institute of Technology. The primary variables in this study are the number of CFRP wraps and the number of post-tensioned strands on the beams. Other parameters were kept as constant as practically possible. The following sections will discuss the details of the specimens, their material properties, test setup, and instrumentation.
Eight beams were cast in two groups for the experimental program. The experimental variables were the number of post-tensioning strands and the number of wraps of carbon fiber polymer. The two groups consisted of beams with 1 and 2 wraps of CFRP. All of the beams had a uniform cross section and similar web reinforcement (8mm diameter bars spaced every 100mm). With these parameters, flexural failure was achieved.
Since this study focuses on flexural capacity, it is ideal to have a greater margin between flexural and shear capacity. Prior to the experiment, the control and test beams were modeled using Response 2000 and hand calculations, and their capacities were estimated.

3.1 Material Properties

3.1.1 Concrete

3.1.1.1 Cement

The concrete mix used in this study adheres to the ACI mix design method. It consists of Ordinary Portland Cement, specifically Ethio OPC 42.5R, with a water-to-cement ratio

of 0.45. The workability of the concrete is classified as Class S4, with a slump range of 160-210mm. To achieve the desired outcome, an admixture called Ultplast G20 was added at a dosage of 2.0% of the cement weight. The concrete exhibited a cubic compressive strength of 23.65MPa after 28 days.
The table below presents the detailed mix design provided by the concrete provider.

PROPORTIONS & WEIGHTS (SSD Conditions):			
Component Description	**Aggregate Percentage**	**Quantities** (Percentages & Weights per 1 mc)	
	%	%	kg/mc
Ethio OPC 42.5R	-	13.3%	330.0
Minerals Capital Cement	-	0.0%	0.0
Ultplast G20	-	0.27%	6.60
Water	-	6.0%	148.5
Crushed Sand (75µm – 4.75mm)	27.6	22.2%	548.8
Natural Sand (75µm – 4.75mm)	18.4	14.8%	365.9
Gravel 4.75 – 25 mm	40	32.2%	795.3
Gravel 5 – 10 mm	14	11.3%	278.4
TOTAL	100	100.0%	2,473.4

Table 3.1: Mix Design of Concrete

3.1.1.2 Fine and Coarse Aggregates

To examine the suitability of the fine and coarse aggregates for the intended application, a series of tests were conducted. The aggregates utilized in this research were determined to be free from contaminants and silt. Subsequently, the properties of both the fine and coarse aggregates were evaluated and found to comply with the ACI-E1-99 specifications. For a comprehensive summary of the material findings, please refer to Appendix 3.

3.1.2 Post Tensioning (Tendons)

A 12.7mm (0.5-inch) diameter strand, with a tested yield strength of 1950 MPa, was utilized[30]. The strands were inserted into ducts to create bonded tendons and anchored at one end of the beams using a wedge block and wedges, as illustrated in Figure 3.1, for the stressing process.
After the beams were cast, the strands were stressed using a hydraulic jacking machine. Subsequently, grouting was performed using a cable and grouting machine, as shown in Figure 3.2 below.

Figure 3.1: Post tensioning Wedge and Anchor Block

Figure 3.2: Grouting Machine, Grouting Tube

3.1.3 CFRP Material

The carbon fiber reinforced polymer (CFRP) utilized in this experimental study was an HM-30 unidirectional (with a braiding angle of 0°) carbon fiber fabric manufactured by Horse Construction[18]. Refer to Figure 3.3 for a visual representation of the CFRP sheet.

Figure 3.3: CFRP Sheet Used

The HM-30 CFRP is fabricated by bonding carbon fibers with epoxy resin adhesive, resulting in a carbon fiber reinforced polymer laminate that is utilized for structural strengthening purposes. This laminate offers exceptional strength and elasticity, along with the added advantages of lightweight construction and superior durability. Its other specifications provided by the manufacturer include;

- ▷ Thickness - 0.167mm
- ▷ Areal Weight - 300g/m^2
- ▷ Appearance - Black fabric[18]

Typical Fiber Properties

Dry Fiber Typical Properties

- ▷ Stand Value of Tensile Strength - 5800 MPa
- ▷ Tensile Elastic Modulus - 255.53 GPa
- ▷ Elongation - 1.60% [18]

Laminated Fiber Typical Properties

- ▷ Stand Value of Tensile Strength (ASTM D3039) - 4840.44 MPa
- ▷ Tensile Elastic Modulus (ASTM D3039) - 255.53 GPa
- ▷ Elongation (ASTM D3039) - 1.95% [18]
- ▷ FRP with Concrete Bonding Strength - $\geq$2.5Mpa, concrete cohesion damage
- ▷ Density - 1.8g/cm^3[18]

3.1.4 Reinforcement bar

Deformed bars with a diameter of 8 and a yield strength of 528.41MPa were utilized.

3.2 Test Specimens

In this study, eight pre-stressed concrete beams measuring 200X200 mm (height x width) and with an overall length of 2000 mm were prepared. The beams were reinforced with 2 dia 8 deformed bars on the bottom surface and 2 dia 8 deformed bars on the top surface. To prevent shear failure, suitable shear reinforcements were incorporated. The stirrups consisted of 8 mm diameter deformed bars, spaced at 100 mm intervals, and covered by 10 mm of clear cover concrete, due to problems with anchor fixation.

The dimensions of the beams and the quantity of non stressed (passive) rebars were deliberately selected to minimize their strength while ensuring realistic parameters, allowing for improved workability, ease of transportation, and avoiding the limits of the testing machines. Likewise, the test setup was also specifically chosen to evaluate the flexural capacity of the test specimens.

3.2.1 The Fabrication of Test Beams

A varying number of 12.7mm PT tendons were positioned 100mm from the soffit of the beam. Strands were placed inside ducts to form bonded tendons, and for the stressing process, they were anchored at one end of the beams using an anchor block and wedges (see Figure 3.1).

The post-tensioned tendons are designed to have a straight profile aligned at the mid-depth of the beams. Holes were made on the side formworks to securely fix the anchors, creating the "Live Ends" of the beams. At the opposite end, the tendon is shaped like an oval, commonly referred to as the "Onion form" (see Figure 3.5). This shape is recommended in general[14] to ensure easy and uniform transmission of prestressing force throughout the beam and to prevent strand slippage during the stressing process, forming the "Dead Ends" of the beams. To achieve this, a dead end machine is used so that all the strands have identical ends.

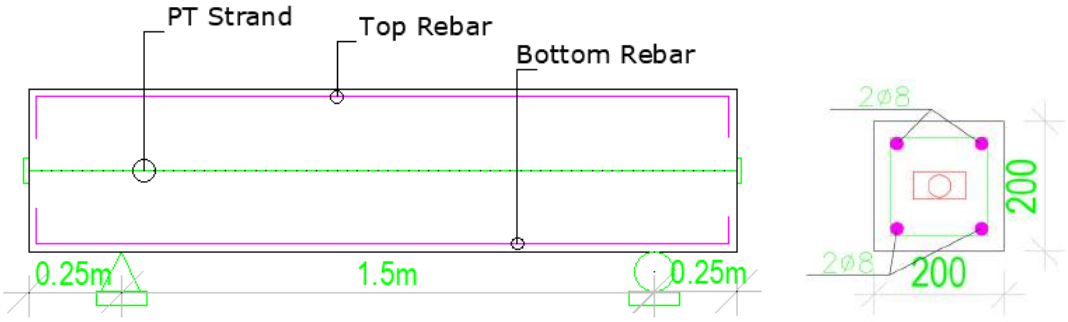

Figure 3.4: Test Beams Cross-Section

Figure 3.5: Onion Form of Dead Ends of Strands

The tendons were tensioned once the concrete reached a strength of 19.79 MPa, which is above the recommended threshold stated in ACI 318[41]. The standard specifies a minimum strength requirement of 17 MPa. The prestressing process continues until the PT tendons reach 80% of their yield stress. After stressing the grouting process takes place using a cementitious material, which is pumped under pressure. The effective span of the beams measure 1500 mm. Figure 3.4 provides a visual representation of the test beam's longitudinal and cross-section.

The Post tensioned beams are pre-damaged. This was achieved experimentally by reducing the number of prestressing tendons used in the beams, similar to how Li et al. conducted their investigation[31]. Hence, in this study, one tendon out of two (50% in the G2B-beam series) and one tendon out of three (33% in the G3B-beam series) were not strained, resulting in anchorage losses of 50% and 33%, respectively. These values are considered to represent prestress levels of 50% and 67%, respectively. The number of strands and prestressing levels were chosen in order to simulate percentage of prestress losses encountered in real post tensioned beams.

Beam series	Beam Designation	No of PT Strands	No of Stressed Strands	CFRP layers	Remarks
1	G2B-20	2	2 (100%)	-	Control beam
	G2B-10	2	1 (50%)	-	Control beam
	G2B-11	2	1 (50%)	1 layer	
	G2B-12	2	1 (50%)	2 layer	
2	G3B-30	3	3 (100%)	-	Control beam
	G3B-20	3	2 (67%)	-	Control beam
	G3B-21	3	2 (67%)	1 layer	
	G3B-22	3	2 (67%)	2 layer	

Table 3.2: Designation of Beam Specimens

The PT beams with two and three strands have been designated as G2B and G3B, respectively. The two-digit numbers in the beam designations have specific meanings. The first digit indicates the number of stressed tendons, while the second digit represents the number of CFRP layers. For example, G2B-12 refers to a PT beam that consists of two strands. The two-digit numeric (12) has the first digit (1) indicating that one strand is stressed, and the second digit (2) denoting the use of two layers of CFRP sheets. For a comprehensive list of the beam specimens and their designations, refer Table 3.2.

CFRP Application

The commonly used technique for FRP strengthening involves the manual application of wet lay-up (also known as hand lay-up) using cold cured adhesive bonding. In this technique, the external reinforcement is bonded to the concrete surface with the fibers oriented as parallel as possible to the direction of principal tensile stresses[19]. For the lamination of CFRP onto the test beams, the hand lay-up technique was employed.

Before applying the carbon fiber, the surface undergoes preparation to eliminate any chemicals or dirt. After preparing the surface and removing dust, any defects in the concrete are repaired. This includes smoothing sharp edges and corners to prevent stress concentrations, also known as polishing[42]. Next, an epoxy-based adhesive (Sika-161) is applied to the concrete, following the manufacturer's recommended mixing instructions[32]. This allows for a mechanical bond before the carbon fiber is installed. Once the epoxy settles, the CFRP (carbon fiber reinforced polymer) is cut to the required dimensions and wrapped around the beams. To eliminate air bubbles trapped at the interfaces, a roller is used for pressing. Figure 3.6 and 3.7 illustrate these processes.

Figure 3.6: Polishing & Primer Application (left to right)

Figure 3.7: Wrapping of CFRP

3.3 Experimental Setup

The beams were positioned on two steel rollers, and a unidirectional monotonic load was applied at the center of the beam until failure. The test setup included a hydraulic jack, a displacement transducer, and surface measurements taken using drawn grids. The full test setup is shown in Figure 3.8 below.

Figure 3.8: Testing Machine Setup

3.3.1 Instrumentation & Data Acquisition

The beam specimen was supported in a simple manner, with a single point load applied at the mid-span. Deflection was measured using a linear variable displacement transducer (LVDT). The experimental setup for the beam specimen is depicted in Figure 3.9. In addition, crack pattern monitoring was employed for beams with no CFRP wrap. Grid patterns were drawn on the side of the test beams to facilitate crack pattern observation. Crack widths were measured throughout the experiment, starting from the load at which crack initiation occurred and at every 10kN increment thereafter.

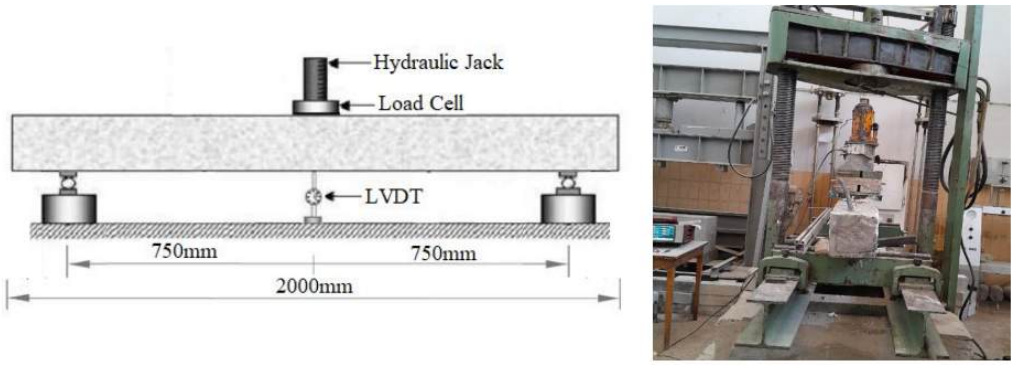

Figure 3.9: Experimental setup with one point loading

Chapter 4

Results and Discussion

This chapter presents the results, observations, and discussions of the experimental program's 8 test beams. The subsequent sections will examine each specimen individually, followed by an analysis of the impact of each experimental variable on the specimen's results. Finally, the observations and results will be addressed in a technically-oriented manner and in accordance with selected code provisions.
During testing, additional weights are placed on top of the beams below the load measuring cell to ensure proper balance, in addition to the load exerted by the load creek. As these weights are not measured by the load cell, they must be manually included. All the weights on the beams not accounted for with the load cell are;

- ▷ Load cell it self - 8.557Kg
- ▷ Weights - 94.715Kg
- ▷ Plate - 3.1Kg

Total additional load on the beams = 106.372Kg = 1043.5093N = 1kN

4.1 Beam Series - 1

The first crack on the initial control beam specimen (G2B-20) occurred at a load of 24kN. This crack, which was a minor flexural crack, had an observed width of 0.04mm. Subsequently, 7 additional cracks formed until the beam ultimately failed at a load of 74kN. The combined width of all the cracks at failure was 19.77mm. It is important to note that the maximum recorded deflection was measured at 5.729mm, although it should be clarified that this is not the ultimate deflection since the LVDT reached its measuring limit. The primary mode of failure for the control beam was flexural, as depicted in Figure 4.1. The cracks developed progressively towards the loading point in correspondence with each load increment.

Figure 4.1: Failure of G2B-20

Figure 4.2 depicts the load deflection diagrams for the G2B beam series. Additionally, Figure 4.3 exhibits the deformed shape, delamination, and rupture/tear out of CFRP laminates observed in the G2B-11 and G2B-12 beam specimens. These findings are consistent with previous research, which has demonstrated that the utilization of CFRP enhances the flexural strength of the beam. Ultimately, debonding of the CFRP and subsequent failure are observed[33].

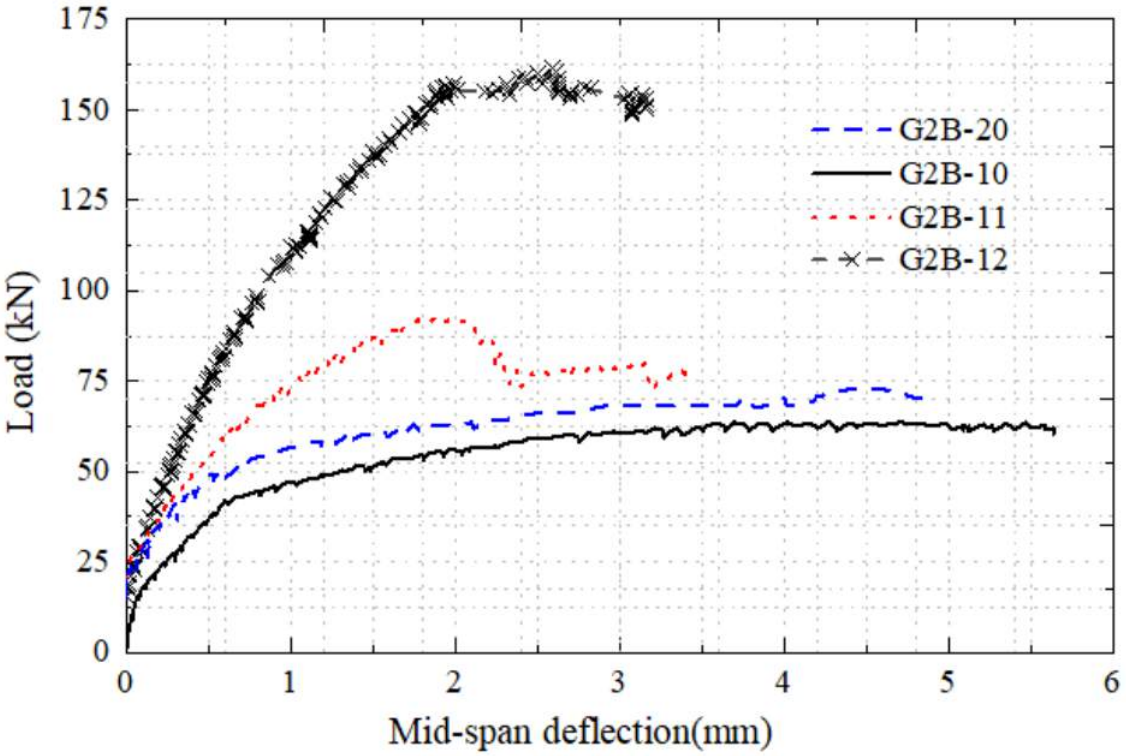

Figure 4.2: Load-deflection curves of control and strengthened beams (Group-1)

As shown in Figure 4.2, when the tendons' prestressing is at 50%, the ultimate capacity of beam (G2B-20) decreased by 13.50%. However, when the member was reinforced with one layer of CFRP sheet, the capacity increased by 45.31% and the deflection decreased by 33.35%. These findings are consistent with the results of a study conducted by a

Chinese university[27], which reported an increase in ultimate load capacity ranging from 31% to 54%. Moreover, the use of two layers of CFRP resulted in a 153% increase in capacity, similar to the study conducted by Askar et al.[22], which reported a load capacity increase of over 100%.
It should be noted that, as illustrated in Figure 4.2, the recorded deflections consistently remained at a value of zero during the initial loading phase. This inconsistency could be attributed to a potential measurement error in the deflection. The LVDT, responsible for measuring the deflections, failed to detect any deflection in the initial stages of the experiments. This could potentially be due to improper positioning of the LVDT, resulting from a lack of direct contact with the beam.

a) b)

Figure 4.3: a) deformed shape of G2B-11 and b) rupture and delamination of CFRP, G2B-12

4.2 Beam Series - 2

The crack pattern and damage to the control beam (G3B-30) are illustrated in Figure 4.4. In the case of a 67% prestressing level, as depicted in Figure 4.5, the ultimate capacity of the beam (G3B-20) is diminished by 19.22% in comparison to the control beam with a 100% prestressing level (G3B-30).

Figure 4.4: Flexural failure of G3B-30

The strengthening of beam G3B-20 through the application of 1 and 2 layers of CFRP sheets yielded a significant increase in the ultimate load capacity by 78.62% and 87.18%

respectively. These findings align with those presented in reference[34], which reported a measured increment of 74.5%. Additionally, the use of one or two layers of CFRP laminates resulted in improved deflection performance, with increases of 25.56% and 23.82% respectively, thereby enhancing the beams' overall serviceability.

As shown in Figure 4.5, the utilization of either 1- or 2-layers of CFRP sheets (G3B-21 and G3B-22) resulted in a nearly equal ultimate load capacity of the beams. However, debonding of the fiber sheets occurred in the latter case. Therefore, in this scenario, the use of 1 layer of CFRP sheet is considered optimal. To prevent the under-utilization of CFRP layers, it is essential to ensure proper anchorage of the CFRP sheets at the beam ends. This prevents debonding failure and enhances the beam's flexural capacity, as demonstrated by experimental investigations conducted by Assad et al.[35].

In this study, the carbon fiber wraps were applied by folding them onto the sides of the beams to enhance anchorage. However, due to the absence of a control beam with a no anchorage system, the exact extent of the anchorage increase resulting from the upward folding of the CFRPs cannot be definitively stated. Numerous alternative anchorage systems have also been developed, including one established by Mashrei et al. [34]. Their research demonstrates that placing the fibers in grooves can effectively enhance the ultimate load carrying capacity. Specifically, their studies revealed that inserting two layers of CFRP sheets into concrete grooves resulted in an increment of up to 103%.

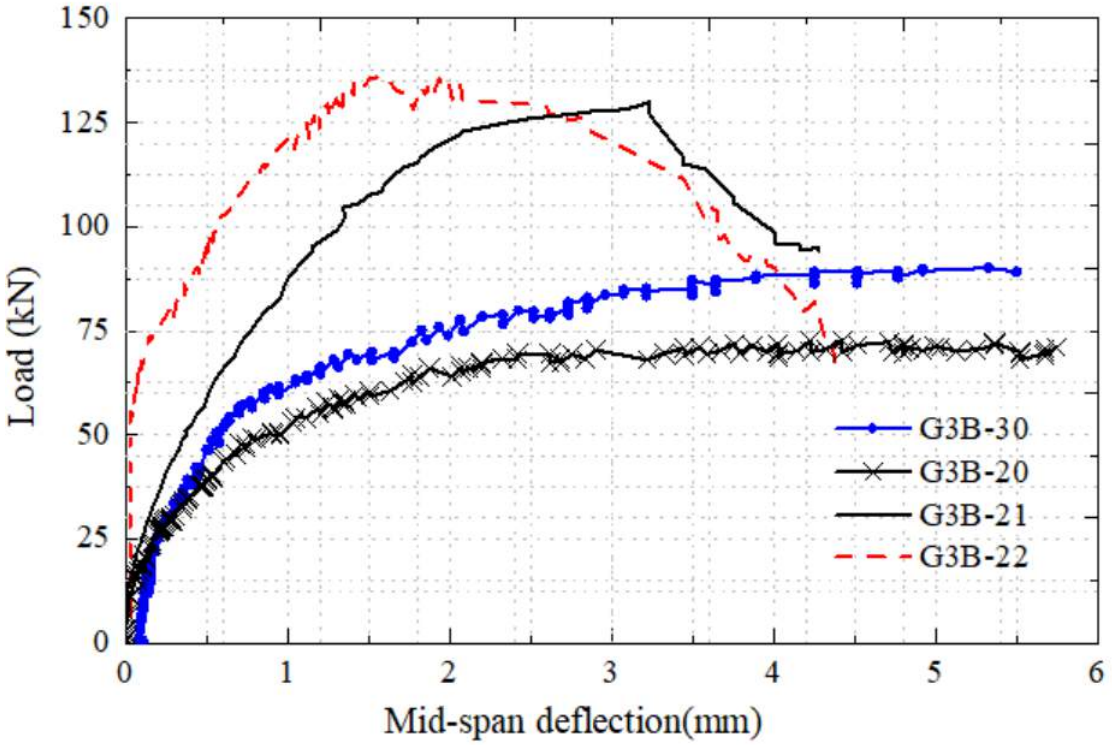

Figure 4.5: Load deflection diagram of G3B beam series

When two layers of CFRP sheets were utilized, the initial cracking load witnessed a

significant increase to 51.32 kN. This shows a large increase of 118.38% when compared to G3B-20, which only achieved a cracking load of 23.5 kN. These results align with the findings of other researchers who have reported a similar or greater than 100% increase in the initial cracking load through the use of EB-CFRP[27, 36]. Furthermore, on average, CFRP laminates minimize beam deflection by 24.7%. Rupture and delamination of G3B-21 and G3B-22 beam specimens are shown in Figure 4.6.

a) b)

Figure 4.6: Rupture and delamination of a) G3B-21 and b) G3B-22

Interestingly, as depicted in Figure 4.7, the utilization of two strands with a prestressing level of 100% (G2B-20, capacity of 75kN) and three strands with a prestressing level of 67% (G3B-20, capacity of 73.8kN) yield nearly identical results, suggesting that the non-prestressed tendon in G3B-20 has a marginal impact (with a 1.6% reduction) on the beam's ultimate capacity and deflection resistance. In the case of G3B-20, the non-prestressed tendon serves as the primary reinforcing bar, as examined by Mortazavi and Shakiba[37]. However, since the non-prestressed tendon is situated closer to the depth of the neutral axis and does not apply pre-compression to the concrete, it diminishes the beam's capacity to withstand external loads. As a result, the utilization of PT tendons becomes less efficient. Therefore, in order to maximize the efficient use of the non-prestressed tendon in G3B-20, it is essential to stress the tendon to the desired prestressing level[38] and/or preventing damage to the beams and making sure the beams do not lose their prestressing force is required[15, 14, 33]. The experimental result of the beams (G2B-20 and G3B-20) is comparable with recent research[39], which showed a 4.4% reduction in ultimate capacity when a PT beam with 2 strands of 65% prestressed ratio (yielded a capacity of 105kN) was compared to a similar beam with 3 strands of 75% prestressed ratio (capacity of 100.3kN was achieved).

Additionally, there was a significant variation in beam load capacity between G2B-12 and G3B-22. It was expected that G3B-22 would have a higher load capacity than G2B-12. However, the opposite result was obtained, with G3B-22 experiencing an 18.90% reduction in load capacity. Despite this, G3B-22 demonstrated good deflection resistance when the same number of CFRP layers were used (2 layers in both cases), albeit with varying numbers of tendons and prestressing levels. As previously discussed, this discrepancy is

likely due to the under-utilization of CFRP fibers and/or inefficient placement of tendon in G3B-22 compared to G2B-12.

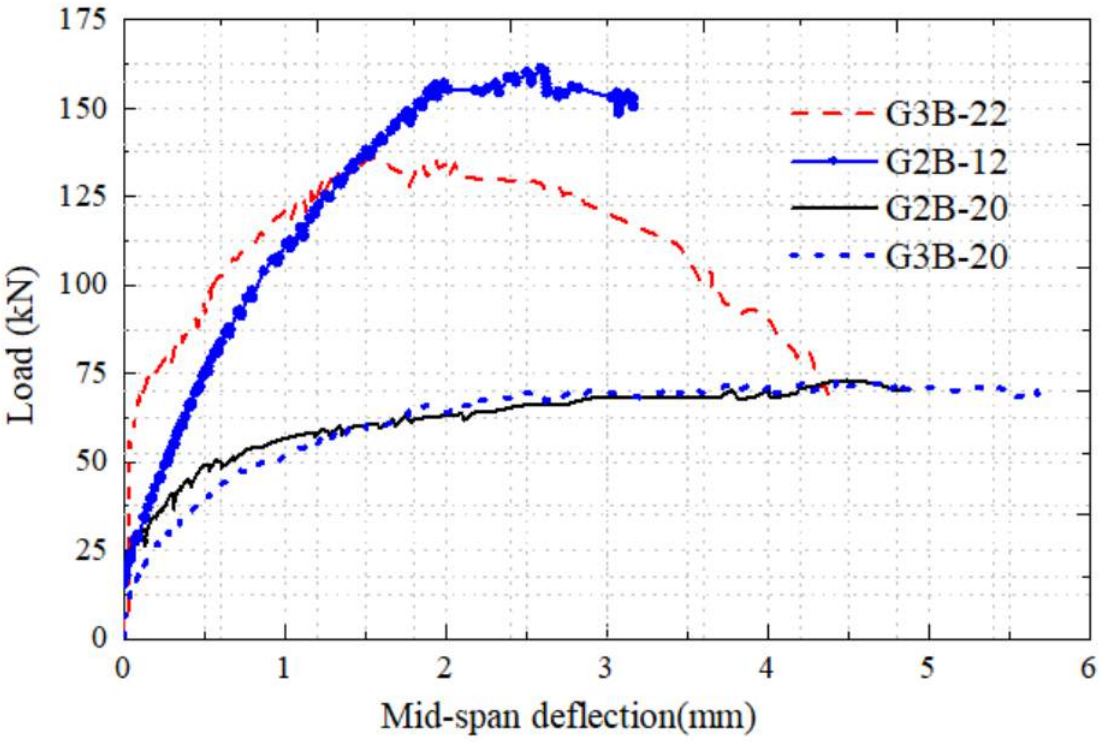

Figure 4.7: Rupture and delamination of a) G3B-21 and b) G3B-22

4.3 Capacity Analysis According to ACI

To determine the theoretical point load capacity of the beams, a capacity analysis was conducted in accordance with ACI 318M. The results were then compared to the experimental data. Table 4.1 provides a comparison between the experimental point load capacities of the beams and the analytical capacities. The general steps of the analysis are outlined here, while a detailed analysis of all beams can be found in Appendix A-1 & A-2.

Calculation Steps

1. Enumerate all the parameters required for the analysis. Ensure that all material strengths are based on the corresponding experimental values without applying any additional factors.

2. Cut the section at mid span where there is maximum moment.

3. Formulate assumptions regarding the yielding and non-yielding behavior of all the reinforcements in the beams, including the compression rebars (located at the top), tension bars (located at the bottom), and prestressing tendons.

4. Calculate the force exerted by each component based on the assumptions made, and utilize the equilibrium equation to determine the force of the concrete.

5. Use the Whitney Stress Block to find "a" which is the depth where there is full compression in the beams & "c" which is the neutral axis depth.

6. Draw the strain diagrams for the beams and verify the assumptions regarding yield as stated in Step 3. If the assumptions are valid, proceed with the next steps. If not, return to Step 3 and repeat the process until the assumptions align with the results.

7. Draw a complete force diagram using the forces found on step 4 and sum moments to determine the moment capacity.

8. Lastly, determine the maximum point load at the mid-span by utilizing the moment found on step 7.

Beam series	Beam Designation	Failure Load (kN)	ACI Point Load Capacity (kN)	Point Load Capacity %	Failure Mode
1	G2B-20	74	69.71	106.15%	Flexural
	G2B-10	64.754	60.06	107.82%	Flexural
	G2B-11	93.121	87.33	106.69%	Flexural
	G2B-12	162.393	149.65	108.52	CFRP Delamination
2	G3B-30	91.109	83.06	109.69%	Flexural
	G3B-20	73.79	69.06	106.85%	Flexural
	G3B-21	125.998	119.51	105.43%	Flexural
	G3B-22	137.85	127.21	108.36%	Flexural/ Delamination

Table 4.1: Result Summary of the Experimental Program

It is apparent that there is a disparity of 5 - 10% between the experimental and analytical point load capacities of the beams, with the analytical values being lower. This discrepancy can be attributed to the inherent lack of 100% accuracy in analysis methods. Despite testing of materials to determine their strength, their actual behavior may deviate from the predicted outcomes. Furthermore, these findings underscore the fact that the ACI analysis method gives a conservative result as it is seen in other researches[46].

4.4 Compression Limit Analysis

Compressive strength refers to the maximum stress a material can withstand before breaking under compression. In the case of normal reinforced concrete (RC) beams,

the bending stress can be expressed as $\delta = \frac{M*y}{I}$, Where δ represents the maximum bending stress at point y along the beam. M denotes the bending moment experienced by the beam, while y represents the greatest distance from the beam's neutral axis to its outermost face. However, when dealing with post-tensioned members, in addition to the bending stress, there is also a pure pre-compression force applied to the beams during the tensioning of the tendons. This compression stress can be determined by dividing the applied force by the cross-sectional area normal to the force. Thus, the equation for the total compressive strength of post-tensioned beams can be derived as follows:

$$\delta = \frac{F}{A} + \frac{M*y}{I}$$

Force (F) represents the applied jacking force on the tendons and is measured at 147kN. The force is exerted on the side dimensions of the beams, which measure 200mm X 200mm. The moment of inertia for a rectangular section is calculated using the formula $I = \frac{b*h^3}{12}$. The maximum compression force, or the furthest distance from the neutral axis; y, is considered to be at the top of the beam. Lastly, the maximum bending moment (M) for a simply supported beam with a point load (P) at the mid-span can be determined using the equation $M = \frac{P*L}{4} + \frac{W*L^2}{8}$. In this equation, P represents the failure loads of the beams (as listed in Table 4.1), and the second term accounts for the self-weight of the beams. Using these calculations, the Maximum Compression Stress in the beams is calculated and presented in Table 4.2 below.

Beam series	Beam Name	Compressive Force at Top Most of Beams	Beam series	Beam Name	Compressive Force at Top most of Beams
1	G2B-20	69.71	2	G3B-30	83.06
	G2B-10	60.06		G3B-20	69.06
	G2B-11	87.33		G3B-21	119.51
	G2B-12	149.65		G3B-22	127.21

Table 4.2: Compressive Forces of Experimental Beams

It is evident that all of the beams at their topmost part exhibit a compressive force that exceeds the tested compressive capacity of the concrete. Therefore, it can be concluded that the upper section of the beams has failed due to compression, which explains the observed concrete crushing in all test beams.

Chapter 5

Conclusion and Recommendation

5.1 Conclusions

The study findings are as follows, based on the measurements, observations, and analysis outlined in the preceding chapters.
The objective of this research was to enhance the flexural strength of damaged post-tensioned beams by utilizing Carbon Fiber Reinforced Polymer (CFRP) wraps. An experimental program was conducted on eight beams, divided into two groups with differing numbers of post-tension strands stressing levels and carbon fiber wraps. Additionally, an analytical investigation was carried out using the ACI-318 code, and a comparison between the experimental and analytical results was performed. Based on the findings from both the experimental and analytical investigations, the following conclusions have been drawn:

- ▷ CFRP sheets have been found to be highly effective. One layer of CFRP sheets can increase load carrying capacity by 45.31% to 78.62%, while two layers can improve flexural capacity by 87.17% to 153%. These findings align well with previous studies[22, 27, 34].

- ▷ The experimental results of this study have also shown that prestressing loss has an impact on beam capacity, with reductions of 13.5% and 19.22% observed at prestressing levels of 50% and 67%, respectively. These findings are in line with previous studies, which have reported the occurrence of diagonal cracks and a decrease in the load-carrying capacity of PT beams due to prestress losses[40].

- ▷ Post tension strands increase the flexural capacity, but also increase the ductility of members. An average of 18.5% increase in deflection capacity was observed per addition of 1 post tension strand.

- ▷ Under-utilization of CFRP fibers and prestressing tendons are found critical and should be considered in design.

- ▷ The pre-compression force in post-tensioned members results in the reduction or closure of existing cracks upon unloading. This effect is particularly significant for narrow cracks that are typically located away from the mid-span of the beam. In the second series of beams, an average crack closure of 64.8% was observed, while in the first series, the average crack recession was 34%. Overall, there was an average of 49.4% closure of cracks. Furthermore, the formation of new cracks was delayed by 118.38%.

- ▷ Delamination patterns also vary with the increase in the number of wraps. When CFRP reaches its flexural capacity, which occurs with a lower number of wraps, it fails in a brittle manner, with the material completely breaking apart. The carbon fiber behaves more like wood in this case. On the other hand, when the number of wraps increases and the flexural capacity is not reached, material failure occurs and the CFRP tears perpendicular to the unidirectional weaves (i.e., along its weaker axis), resulting in complete delamination from the beam. Therefore, it can be concluded that increasing the number of wraps of CFRP on beams significantly increases the likelihood of delamination failure. Also using multi-directional (double-weaved) CFRP, which provides increased capacity in both directions, could greatly enhance the beam's load-bearing capacity.

- ▷ It can be concluded that post-tensioned beams respond to the strengthening process using CFRP in a manner similar to reinforced concrete (RC) beams. The moment capacity of post-tensioned beams can increase by a range of 15 to 90%, depending on the application method[44, 34]. However, there may be slight variations in deflection and crack patterns.

5.2 Recommendations

The following recommendations are made based on the results and analysis conducted:

1. Conduct a further study on beams strengthened with bidirectional (double weaved) Carbon Fiber Polymer.
2. Investigate the effect of other types of reinforcing polymers such as Glass or Aramid fibers on post tension members.
3. Due to limitations, only one point loading test was performed in this study. However, further investigation using more advanced methods such as two point, three point, or cyclic loading tests can be conducted.
4. Clear cover is taken as 10mm in this study. It is recommended to conduct further studies with higher clear covers.
5. Conduct further investigation into the recession of cracks in post tensioned members after unloading.
6. Perform further analytical investigations using other national codes and compare the results.
7. Due to unavailability of strain measuring equipment in the country, strain measurements were not conducted during the experiment. It is therefore recommended to conduct strain measurements on members such as the ones in this paper. This will allow for a detailed investigation on the stresses in the beams and how the CFRP affects the stress development in these members.
8. Further investigate beams with a higher number of wraps, as well as beams with higher concrete strength, in order to determine how the rate of increase in capacity changes with each additional wrap.
9. Conduct further investigation on the relationship between ductility and the number of wraps of fiber polymers.

Reference

[1] Konstantin Kovler, V. Chernov (2009). Types of Damage in Concrete Structures. Israel Institute of Technology.

[2] ACI-ASCE Committee 423 (1999). ACI 423.5R-99: State-of-the-Art Report on Partially Prestressed Concrete, American Concrete Institute.

[3] Hewson NR. (2003). Prestressed Concrete Bridges: Design and Construction. Heron Quay, London, Thomas Telford Publishing.

[4] Nishikant Dash (2009). Strengthening of Reinforced Concrete Beams Using Glass Fiber Reinforced Polymer Composites. MSc Thesis, National Institute Of Technology Rourkela.

[5] Owen Rosenboom, Tare K. Hassan, Sami Rizkalla (2006). Flexural behavior of aged prestressed concrete girders strengthened with various FRP systems. North Carolina State University.

[6] R. Balamuralikrishnan1 and C. Antony Jeyasehar (TOCIEJ 2009). Flexural Behavior of RC Beams Strengthened with Carbon Fiber Reinforced Polymer (CFRP) Fabrics. Tamilnadu, India, Annamalai University.

[7] Bondy, K. (2012). Two-Way Post-Tension Slabs with Bonded Tendons. PTI Journal.

[8] Len Hollaway & Jin-Guang Teng (2008). Strengthening and Rehabilitation of Civil Infrastructures Using Fiber-Reinforced Polymer (FRP) Composites. Cambridge, England, Woodhead Publishing Limited.

[9] FIB, Bulletin 14, Task Group 9.3 (July 2001), "Design and use of externally bonded fiber reinforced polymer reinforcement (FRP EBR) for reinforced concrete structures'.

[10] Wondmagegne Dagne (2019). Post-Tensioning Concrete Flat Slab Design for Buildings, Construction Practice and Prospects in Ethiopia. MSc Thesis, Addis Ababa Institute of Technology (AAiT).

[11] K. Dirk Bondy & Bryan Allred (2016). Post-Tensioned Concrete Principles and Practice, Third Edition. California, USA, Lulu Publishing Services.

[12] http://www.tensionedconcrete.com.au/post-tensioning-services/

[13] Stacy Johnson (2006). Analytical Modeling of Fiber Reinforced Post-Tensioned Concrete Anchorage Zones. MSc Thesis, The Florida State University Famu-fsu College of Engineering

[14] Massoud Sofi, Daksh Baweja & Elvira E. (2011). Numerical Simulation of Failure Mechanisms of a Typical Dead End Anchorage of Post-Tensioned Suspended Slabs.

[15] Kamal Tawfiq & Brenda Robinson (2008). Post-Tensioned Bridge Girder Anchorage Zone Enhancement with Fiber Reinforced Concrete (FRC). Department of Transportation, Florida.

[16] Construction Durability Engineers (CDE) (2023). Evaluation of Corrosion Risk for Post Tensioned (PT) Slab. https://www.linkedin.com/pulse/evaluation-corrosion-risk-post-tensioned/.

[17] Abel Gebretsadik & Mice (UK) (2021). Strengthening concrete structures with Fiber Reinforced Polymer (FRP) and Its future prospect in Ethiopia. AA, Ethiopia and United Kingdom.

[18] Shanghai Horse Construction Product Data Sheet (2019). Horse HM-30 Unidirectional Carbon Fiber Fabric For Strengthening. 1228 Jiangchang Rd, Shanghai, China.

[19] Abenezer Negussie (2018). Enhancement of the Flexural Behavior of CFRP Strengthened RC Beams in Medium and Low-Grade Concrete. MSc Thesis, Addis Ababa Institute of Technology (AAiT).

[20] Jamal A. Abdalla, Abubakr Mohammed, Rami A. Hawileh (2020). Flexural Strengthening of Reinforced Concrete Beams with Externally Bonded Hybrid Systems. American University of Sharjah, Sharjah, UAE.

[21] Hebah Al-zu'bi, Mu'tasim Abdel-Jaber, Hasan Katkhuda (2022). Flexural Strengthening of Reinforced Concrete Beams with Variable Compressive Strength Using Near-Surface Mounted Carbon-Fiber-Reinforced Polymer Strips [NSM-CFRP]. The University of Jordan, Amman 11942, Jordan.

[22] Mand Kamal Askar, Ali Falyeh Hassan, Yaman S.S Al-Kamaki (2022). Flexural and shear strengthening of reinforced concrete beams using FRP composites: A state of the art. University of Duhok (UoD), Kurdistan Region, Iraq.

[23] Ali Saribiyik, Naci Caglar (2016). Flexural Strengthening of RC Beams with low-strength concrete using GFRP and CFRP.

[24] Adi Setiawan, Sumargo Sumargo, Mardiana Oesman (2021). The Behavior of Low Strength Concrete Beams Reinforced with Carbon Fiber Reinforced Polymer Under Cyclic Loading. Jenderal Achmad Yani University, Indonesia.

[25] Tarek Hassan, Sami Rizkalla (2002). Flexural Strengthening of Prestressed Bridge Slabs with FRP Systems. University of Manitoba, Winnipeg, Manitoba, Canada.

[26] Deng J, Rashid K, Li X, Xie Y, Chen S (2020). Comparative study on prestress loss and flexural performance of rectangular and T beam strengthened by prestressing CFRP plate. Guangzhou University, China.

[27] L.L. Chen, X.H. Qiang & X. Jiang, P. Liu (2023). Flexural behavior of prestressed concrete beams strengthened with external CFRP tendons. Tongji University, Shanghai, China

[28] Yail J. Kim, Chen Shi and Mark F. Green (2008). Ductility and Cracking Behavior of Prestressed Concrete Beams Strengthened with Prestressed CFRP Sheets. Journal Of Composites For Construction, ASCE, America.

[29] T.P. Meikandaan, M.Hemapriya (2017). Use of Glass FRP Sheets as External Flexural Reinforcement In RCC Beam. Bharath University, Chennai, Tamilnadu, India

[30] Qingdao Global Overseas IMP & EXP CO., LTD (2023). Mill Test Certificate. Qingdao, China.

[31] Fangyuan Li ,Wenhao Li, Shaohui Lu, and Yin Shen (2019). Development of a Prestressing CFRP Laminate Anchorage System and Bridge Strengthening Application. Tongji University, China.

[32] (2019) Product Data Sheet, Sikafloor®-161.

[33] Young Chan You, Ki Sun Choi, Junhee Kim (2012). An experimental investigation on flexural behavior of RC beams strengthened with prestressed CFRP strips using a durable anchorage system. Yonsei University, South Korea.

[34] Mohammed. A. Mashrei, Jamal. S. Makki, Ali A. Sultan (2019). Flexural Strengthening of Reinforced Concrete Beams Using Carbon Fiber Reinforced Polymer (CFRP) Sheets with Grooves. University of Thi-Qar, Iraq.

[35] Maha Assad, Rami A. Hawileh, Jamal A. Abdalla (2024). Flexural strengthening of reinforced concrete beams with CFRP laminates and spike anchors. American University of Sharjah, Sharjah, UAE.

[36] Yihua Zeng, Xinghua Li, Amira Hamdy Ali Ahmed and Gang Wu (2020). Comparative study on the flexural strengthening of RC beams using EB CFRP sheets, NSM CFRP bars, P-SWRs, and their combinations. Nanjing, Jiangsu 210096, China.

[37] Seyed Mohammad Reza Mortazavi, Milad Shakiba (2022). Experimental Study on RC Deep Beams with Non-Prestressed Tendons as Main Reinforcement. Shahid Rajaee Teacher Training University, Tehran, Iran.

[38] Antoine E. Naaman (2012). Prestressed Concrete Analysis And Design: Fundamentals, Third Edition. University of Michigan, Ann Arbor

[39] Dong Chen, Bin Zeng, Qing Xu, Xiaoda Xu and Man Xu (2024). Effects of Prestressing Magnitude and Position on Seismic Performance of Unbonded Prestressed Concrete Beams. Xi'an University of Architecture and Technology, Xi'an 710055, China.

[40] Xudong Shao, Rensheng Pan, Hua Zhao, Zixuan Shao (2014). Prestress Loss of a New Vertical Prestressing Anchorage System on Concrete Box-Girder Webs. American Society of Civil Engineers (ASCE), America.

[41] ACI Committee 318. (2019) Building Code Requirements for Structural Concrete (ACI 318–2019) and Commentary (ACI 318–2019). American Concrete Institute.

[42] ACI Committee (July 2008). ACI 440.2 R-08: Guide for the Design and Construction of Externally Bonded FRP Systems for Strengthening Concrete Structures, American Co ncrete Institute

[43] Aalami, B. (1994). Unbonded and Bonded Post-Tensioning Systems in Building Construction: A Design and Performance Review. PTI Technical Notes, 5th ser.

[44] Asad ur Rehman Khan (2013). Behavior of Reinforced Concrete Beams Strengthened by CFRP Wraps with and without End Anchorages. NED University of Engineering & Technology, Karachi-75270, Pakistan.

[45] ACI 440.2 R-17 (May 2017), Guide for the Design and Construction of Externally Bonded FRP Systems for Strengthening Concrete Structures, American Concrete Institute.

[46] Wisena Perceka, Wen-Cheng Liao & Yung-Fu Wu (2019). Shear Strength Prediction Equations and Experimental Study of High Strength Steel Fiber-Reinforced Concrete Beams with Different Shear Span-to-Depth Ratios. Parahyangan Catholic University, Indonesia.

Appendix A

Appendices

A.1 Section Analysis of Control Beams G2B-20 and G3B-20

1. Beam Series 1 - G2B-20

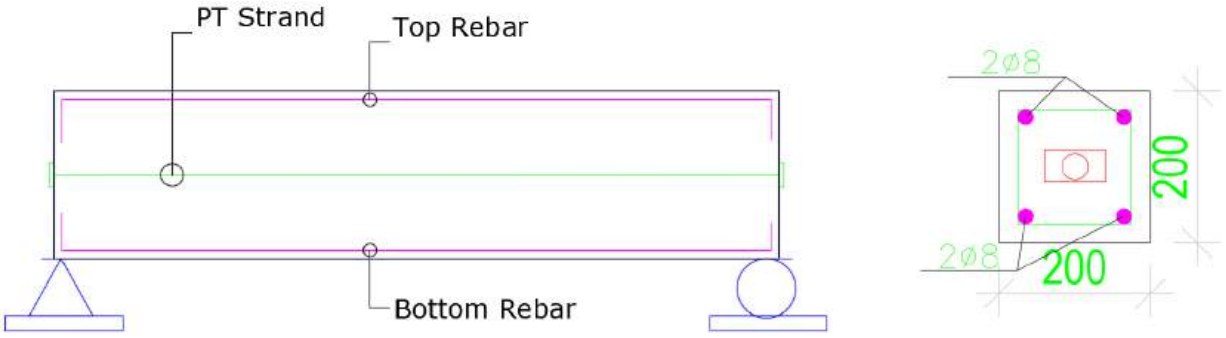

Two Post tension Strands + Two Strands Stressed

Material Properties

$f'_c = 23.66Mpa$

$f_{pu} = 1950Mpa$

$f_y = 528.41Mpa$

$A_{ps} = 2 * 98.7mm^2 = 197.4mm^2$

$A_{st} = A_{sc} = 2 * 50.24mm^2 = 100.48mm^2$,

2 dia 8, Top & Bottom

The maximum usable moment capacity at mid span and the maximum mid span factored point load are as follows;

*Straight tendon profile with tendon placed at Mid depth of the beam ($d_p = 100mm$)

$f_{ps} = 1950MPa$, Ultimate tested strength of the post tensioning and no material factors are used.

Cut a section at mid span.

Different assumptions are checked but the final arrangement is presented here. i.e Assumptions are;

Compression steel yields; Tension steel Not yield.

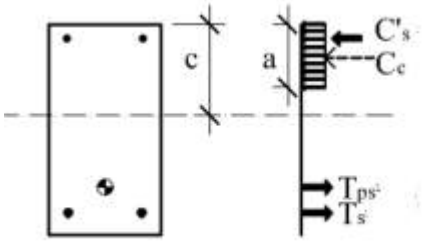

C'$_s$= 100.48mm^2*(528.41MPa) = 53.094kN
T$_{ps}$ = 197.4mm^2*(1950MPa) = 384.93kN
T$_s$= 100.48mm^2*(528.41MPa) = 53.094kN
Using equilibrium, solve for the concrete force C$_c$
C$_c$= T$_{ps}$+ T$_s$- C'$_s$= 384.93+53.094-53.094 = 384.93kN
Now use the Whitney Stress Block to find "a" & "c"
a = $\frac{C_c}{0.85 f'_c b} = \frac{384.93KN}{0.85*23.66MPa*200mm} = 95.701mm$
c = $\frac{a}{\beta_1} = \frac{95.701}{0.85} = 112.5898mm$
Draw the strain diagram and check to see if the compression steel is yielding.
$\xi'_s = \frac{0.003*(c-d'c)}{c} = 0.002414 > 0.002$(Compression Steel has yielded)
$\xi_s = \frac{0.003*(d'-c)}{c} = 0.001743 > 0.002$ (Tension Steel not Yielded, member is not tension controlled)
$M_n = 53.094kN + (178 - 22)mm + 384.93kN * (178 - 67.95243/2)mm - 384.93kN * (78mm) = 35.3566kNmm$
Find maximum factored point load at mid span, only uniform load is the beam's weight itself
w$_u$= (25KN/m^2* 200mm * 200mm)/10^6= 1KN/m
M$_u$= $\frac{W_u L^2}{8} + \frac{P_u L}{4} = \frac{1KN/m*(2m^2)}{8} + \frac{P_u 2m}{4} = 0.5KNm + 0.5P = 35.3566$
P$_u$= 69.7132KN Point Load

2. Beam Series 2 - G3B-20

Three Post tension Strands + Two Strands Stressed

Material Properties

$f'_c = 24.6MPa$
$f_{pu} = 1950MPa$
$f_y = 528.41MPa$
$A_{ps} = 2 * 98.7mm^2 = 197.4mm^2$(Stressed Strands)
$A_{ps} = 1 * 98.7mm^2 = 98.7mm^2$(Not Pre-stressed Strand)
$A_{st} = A_{sc} = 2 * 50.24mm^2 = 100.48mm^2$,
2 dia 8, Top & Bottom

The Non-Prestressed post tension strand is treated as a passive rebar as it does not have pre-stressing force inside it.
The maximum usable moment capacity at mid span and the maximum mid span factored point load are as follows;
*Straight tendon profile with tendon placed at Mid depth of the beam ($d_p = 100mm$)
$f_{ps} = 1950MPa$, Ultimate tested strength of the post tensioning and no material factors are used.
Cut a section at mid span.
Different assumptions are checked but the final arrangement is presented here. i.e Assumptions are;
Compression steel yields; Tension steel also yields
C'$_s$= 100.48mm^2*(528.41MPa) = 53.094kN (Force of the Compression Steel)
T$_{ps}$ = 197.4mm^2*(1950MPa) = 384.93KN (Force of the Stressed Post Tension)
T$_s$= 100.48mm^2*(528.41MPa) = 53.094kN (Force of the Tension Steel)
T$_{ps,NS}$= 98.7mm^2* (0.8*1950MPa) = 153.972kN (Force of the Not-Stressed Post Tension Strand)
Using equilibrium, solve for the concrete force C$_c$
C$_c$= -T$_{ps}$-T$_{ps,NS}$+ T$_s$- C'$_s$= $-384.93 - 153.972 + 53.094 - 53.094 = -485.808kN$
Now use the Whitney Stress Block to find "a" & "c"
a = $\frac{C_c}{0.85f'_cb} = \frac{485.808KN}{0.85*24.6MPa*200mm} = 112.2205mm$
c = $\frac{a}{\beta_1} = \frac{110.1115}{0.85} = 132.0241mm$
Draw the strain diagram and check to see if the compression steel is yielding.
$\xi'_s = \frac{0.003*(c-d')}{c} = 0.002517 > 0.002$(Compression Steel has yielded)
$\xi_s = \frac{0.003*(d'-c)}{c} = 0.00104 < 0.002$ (Tension Steel not Yielded, member is not tension controlled)
$\xi_{s,pt} = \frac{0.003*(c-(\frac{h}{2}))}{c} = 0.000728 < 0.002$ (Not Stressed Post tension Strand has not yielded)
Draw the complete force diagram and sum moments to determine the moment capacity
$M_n = (53.094kN*(178mm-22mm)+485.808kN*(178mm-116.1664mm/2)-384.93kN*(78mm) - 153.972*(78mm) = 35.03$
Find maximum factored point load at mid span
Since, the only uniform load is the beam's weight itself
w$_u$= (25kN/m^2* 200mm * 200mm)/10^6= 1kN/m
M$_u$= $\frac{W_uL^2}{8} + \frac{P_uL}{4} = \frac{3KN/m*(2m^2)}{8} + \frac{P_u2m}{4} = 0.5kNm + 0.5P = 35.03$
P$_u$= 69.06kN Point Load

A.2 Section Analysis of CFRP Wrapped Test Beams (G2B-11 and G3B-22)

1. Beam Series 1 - G2B-11

Two post tension Strands + One Strand Stressed + 1 Wrap of CFRP

Material Properties

$f'_c = 25.54MPa$

$f_{pu} = 1950MPa$

$f_y = 528.41MPa$

$A_{ps} = 1 * 98.7mm^2 = 98.7mm^2$(Stressed Strands)

$A_{ps} = 1 * 98.7mm^2 = 98.7mm^2$(Not Pre-stressed Strand)

$A_{st} = A_{sc} = 2 * 50.24mm^2 = 100.48mm^2$,

2 dia 8, Top & Bottom

CFRP

Tensile strength of FRP, (ff) = 5804 MPa (Stand Value of Tensile Strength is Used)

Modulus of Elasticity, Ef = 259.251 GPa

Rupture strain of FRP reinforcement = 0.016

Section Property

Thickness (t_f) = 0.167 mm

Width (B_f) = 200 mm

Cross-sectional Area (Af) = 33.4 mm^2

Section Analysis According to ACI-440-2R-17

The section analysis assumes perfect bonding and linear strain distribution along the section of the beam.

Depth of the FRP from the top (d_f) = 200+(0.167/2) = 200.0835 mm taken as 200mm

Depth of the bottom reinforcement from the top (d_1) = 178mm

Depth of the top reinforcement from the top (d') = 22mm

Because the CFRP that is laminated to the side (for Anchorage) also has a small effect on the capacity increase of the beam we account it by considering the confinement effect it has on the beam. Max confinement pressure f_l is calculated with the equation 12.1h of ACI_440_2R_17[45].

$$f_l = \frac{2E_f n t_f \varepsilon_{fe}}{D} = \frac{2 * (259.251GPa) * 1 * 0.167mm * 0.0189}{282.84mm^2} = 0.005786N/mm^3$$

Ultimate strain is taken as the effective CFRP ε_{fe} and the equivalent diameter of confinement for Non-rectangular sections D is taken as $D = \sqrt{b^2 + h^2}$[45].

Pressure is then converted to applied force by multiplying it with the volume it acts on and included in the equilibrium equation assuming the force acts at the center of upward bent CFRP. Hence force of the confinement F_c is given as

$F_c = 0.005786N/mm^3 * (200mm * 150mm * 2000mm) = 347,160N$

$F_c = 347.16KN$

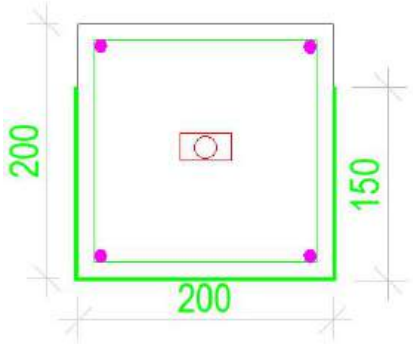

Assumption

The section analysis assumes perfect bonding and linear strain distribution along the section of a rectangular beam. Several assumptions are iterated and the final result is presented here;

Concrete crushes at 3‰=0.003

Bottom reinforcement yield, $\xi s1 > \xi y = 2‰ = 0.002$

Top reinforcement yield, $\xi s' > \xi y = 0.002$

The not stressed tendon does not yield $\xi s_{pt,NS} < \xi y = 0.0095$

The strain in the fiber is less than the ultimate strain, $\xi f < \xi fu = 18.9‰ = 0.0189$

Calculation

Use ultimate strength of posttension strand same as previous beams.

f_{ps} = 1950MPa

Cut a section at mid span.

C'_s= 100.48mm^2*(528.41MPa) = 53.094kN (Force of the Compression Steel)

T_{ps} = 98.7mm^2*(1950MPa) = 192.465kN (Force of the Stressed Post Tension)

T_s= 100.48mm^2*(528.41MPa) = 53.094kN (Force of the Tension Steel)

$T_{ps,NS}$= $A_{pt,NS}$*$E_{pt} * \xi_{pt}$

C_c= 0.85*f'_c*b*a

Now use the summation of forces in the X to solve a quadratic equation and find "c"

c =134.8307mm

a = 0.85*c = 114.6061mm

Draw the strain diagram and check to see if the compression steel is yielding.

$\xi'_s = \frac{0.003*(c-d')}{c} = 0.00251 > 0.002$(Compression Steel has yielded)

$\xi_s = \frac{0.003*(d'-c)}{c} = 0.0053 > 0.002$ (Tension Steel has yielded)

$\xi_{s,pt} = \frac{0.003*(c-(\frac{h}{2}))}{c} = 0.000775 < 0.0095$ (Not Stressed Post tension Strand has not yielded)

$\xi_{s,cf} = \frac{0.003*(D-c)}{c} = 0.00145 < 0.0189$ (CFRP has not yielded)

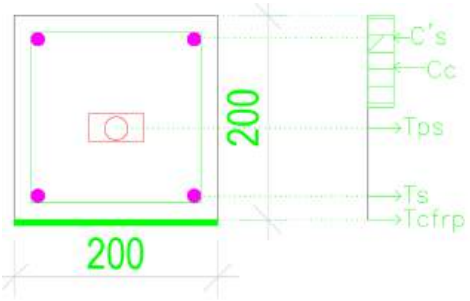

Draw the complete force diagram and sum moments to determine the moment capacity, Mn

M_n = (C'$_s$)*156mm + C_c*141.7mm - T_{ps}*78mm + T_{cfrp}*22mm = 0

M_n = 27.423kN-m

Find maximum factored point load at mid span

Since, the only uniform load is the beam's weight itself and is similar to all the previous beams

w_u= 1KN/m

M_u= $0.5KNm + 0.5P = 44.167$

P_u= 87.33407KN Point Load

2. Beam Series 2 - G3B-22

Three post tension Strands + Two Strands Stressed + 2 Wrap of CFRP

Material Properties

$f'_c = 25.54MPa$

$f_{pu} = 1950MPa$

$f_y = 528.41MPa$

$A_{ps} = 2 * 98.7mm^2 = 197.4mm^2$(Stressed Strands)

$A_{ps} = 1 * 98.7mm^2 = 98.7mm^2$(Not Pre-stressed Strand)

$A_{st} = A_{sc} = 2 * 50.24mm^2 = 100.48mm^2$,

2 dia 8, Top & Bottom

CFRP

Tensile strength of FRP, (ff) = 5804 MPa

Modulus of Elasticity, Ef = 259.251 GPa

Rupture strain of FRP reinforcement = 0.016

Section Property

Thickness (t_f) = 0.167 mm

Width (B_f) = 200 mm

Cross-sectional Area (Af) = 66.8 mm^2

Section Analysis According to ACI-440-2R-17

The section analysis assumes perfect bonding and linear strain distribution along the section of the beam.
Depth of the FRP from the top (d_f) = 200+(0.167/2) = 200.0835 mm taken as 200mm
Depth of the bottom reinforcement from the top (d_1) = 178mm
Depth of the top reinforcement from the top (d') = 22mm
Assumption
The section analysis assumes perfect bonding and linear strain distribution along the section of a rectangular beam. Several assumptions are iterated and the final result is presented here;
Concrete crushes at 3‰=0.003
Bottom reinforcement yield, $\xi s1 > \xi y = 2‰ = 0.002$
Top reinforcement yield, $\xi s' > \xi y = 0.002$
The not stressed tendon does not yield $\xi s_{pt,NS} < \xi y = 0.0095$
The strain in the fiber is less than the ultimate strain, $\xi f < \xi fu = 18.9‰ = 0.0189$
Calculation
f_{ps} = 1950MPa
Cut a section at mid span.
C'_s= 100.48mm^2*(528.41MPa) = 53.094kN (Force of the Compression Steel)
T_{ps} = 98.7mm^2*(1950MPa) = 192.465kN (Force of the Stressed Post Tension)
T_s= 100.48mm^2*(528.41MPa) = 53.094kN (Force of the Tension Steel)
$T_{ps,NS}$= $A_{pt,NS}$*E_{pt} * ξ_{pt}
C_c= 0.85*f'_c*b*a
Now use the summation of forces in the X to solve a quadratic equation and find "c"
c =88mm
a = 0.85*c = 74.8mm
Draw the strain diagram and check to see if the compression steel is yielding.
$\xi'_s = \frac{0.003*(c-d')}{c} = 0.00225 > 0.002$(Compression Steel has yielded)
$\xi_s = \frac{0.003*(d'-c)}{c} = 0.0031 > 0.002$ (Tension Steel has yielded)
$\xi_{s,pt} = \frac{0.003*(c-(\frac{h}{2})}{c} = 0.0004 < 0.0095$ (Not Stressed Post tension Strand has not yielded)
$\xi_{s,cf} = \frac{0.003*(D-c)}{c} = 0.0038 < 0.0189$ (CFRP has not yielded)
Draw a complete force diagram and sum moments to determine the moment capacity
M_n = (C'_s)*156mm + C_c*141.7mm - T_{ps}*78mm + T_{cfrp}*22mm = 0
M_n = 64.3823kN-m
Find maximum factored point load at mid span
w_u= 1kN/m
M_u= $0.5kNm + 0.5P = 65.3823$
P_u= 127.7647kN Point Load

A.3 Detailed Material Test Results From the Experimental Program

▷ Absorption Capacity = 4.93%

▷ Average Specific Gravity (A.s.g) = 2.853 gr/cm^3

▷ Bulk Specific Gravity (B.s.g) = 2.625 gr/cm^3

▷ Silt Content = 2%

▷ Sieve Analysis

Natural Sand (75μm-4.75mm)			
Initial Dry Weight gr.		2691	
Sieve Size, mm	Cumulative Retained, gr	Cumulative Retained, %	Cumulative Pass, %
6.3	0	0	0
4.75	75	2-8	97.2
2.36	103	3-8	96.2
1.18	120	4-5	95.5
0.6	158	5.9	94.1
0.3	632	23.5	76.5
0.15	1780	66.1	33.9
0.075	2470	91.8	8.2
pan			

Table A.1: Sieve Analysis of Natural Sand

Crushed Sand (75μm-4.75mm)			
Initial Dry Weight gr.		2915	
Sieve Size, mm	Cumulative Retained, gr	Cumulative Retained, %	Cumulative Pass, %
6.3	0	0	0
4.75	471	16.2	83.8
2.36	1422	48.8	51.2
1.18	1863	63.9	36.1
0.6	2147	73.7	26.3
0.3	2390	82.0	18.0
0.15	2514	86.2	13.8
0.075	2638	90.5	9.5
pan			

Table A.2: Sieve Analysis of Crushed Sand

Crushed Gravel (9.5mm - 25mm)			
Initial Dry Weight gr.		3651	
Sieve Size, mm	Cumulative Retained, gr	Cumulative Retained, %	Cumulative Pass, %
37.5	0	0	0
25	231	6.3	93.7
19	1907	52.2	47.8
12.5	-	-	-
9.5	3619	99.1	0.9
6.3	-	-	-
4.75	3644	99.8	0.2
2.36	3645	99.8	0.2
pan			

Table A.3: Particle Size Analysis of Gravel (9.5mm - 25mm)

Crushed Gravel (4.75mm - 9.5mm)			
Initial Dry Weight gr.		3034	
Sieve Size, mm	Cumulative Retained, gr	Cumulative Retained, %	Cumulative Pass, %
12.5	0	0	0
9.5	577	19.0	81.0
6.30	-	-	-
4.75	2946	97.1	2.9
2.36	2993	98.6	1.4
1.18	2999	98.8	1.2
0.6	3002	98.9	1.1
0.3	3006	99.1	0.9
pan			

Table A.4: Particle Size Analysis of Gravel (4.75mm - 9.5mm)

A.4 Detailed Experiment Results

A.4.1 Beam Series - 1

A.4.1.1 Beam Series 1 - Control Beam 1 (G2B-20)

Crack Summary Table A.5 depicts when the cracks first appeared on the beam along with their crack width's every 10kN increase until their failure.

Load (kN)	Crack Width (Right Side)							
	Crack 0	Crack 1	Crack 2			Crack 3		Crack 4
			2	2'	2"	3	3'	
24	0.04mm							
30	0.04mm	0.04mm						
40	0.2mm	0.2mm	0.08mm	0.1mm	0.08mm			
50	0.3mm	0.2mm	0.25mm	0.2mm	0.3mm	0.04mm	0.04mm	
60	1.2mm	0.2mm	1mm	0.2mm	2mm	0.1mm	0.08mm	
70	2mm	0.45mm	7mm	0.25mm	4mm	0.1mm	0.08mm	
74	3mm	0.5mm	10mm	0.15mm	4mm	0.04mm	0.08mm	2mm

Table A.5: G2B-20 Crack Summary

Table A.6 summarizes all the crack width's after the beam is unloaded and removed from the testing machine.

	Crack Width After Unloading							
	Crack 0	Crack 1	Crack 2			Crack 3		Crack 4
			2	2'	2"	3	3'	
Unloaded	1.4mm	0.65mm	Invalid	0.06mm	3mm	0.04mm	0mm	Invalid
%age Decrease	***	23%	–	60%	25%	0%	100%	–

Table A.6: G2B-20 Crack Summary After Unloading

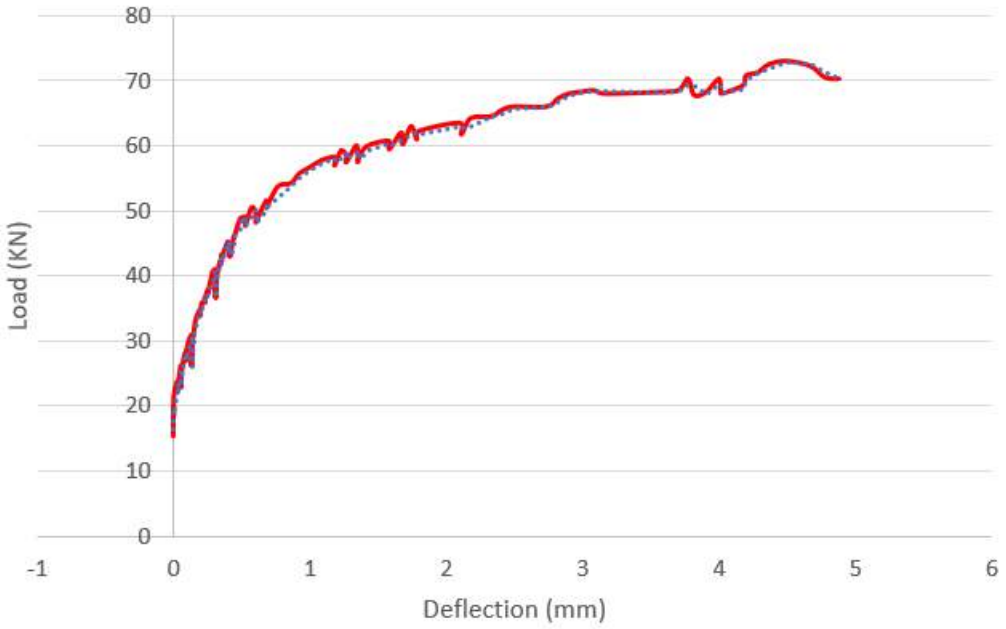

Figure A.1: Filtered Load Vs Deflection of G2B-20

Figure A.2: Close up on the Failure State of G2B-20

A.4.1.2 Beam Series 1 - Control Beam Two (G2B-10)

Crack Summary Table A.7 summarizes the sizes of the cracks on the beam after failure on both the right and left side.

Load	Crack Width (Right Side)				
(kN)	Crack 0	Crack 0'	Crack 1	Crack 2	Crack 3
64.754	1mm	0.5cm/5mm	1.3mm	2.5mm	3.5mm

Load (kN)	Crack Width (Left Side)					
	Crack 0	Crack 0'	Crack 0"	Crack 1	Crack 2	Crack 2'
64.754	0.5cm/5mm	0.7cm/7mm	0.2cm/2mm	1.5mm	0.6cm/6mm	0.4mm

Table A.7: G2B-10 Crack Summary

Table A.8 summarizes all the crack width's after the beam is unloaded and removed from the testing machine.

	Crack Width (Right Side)				
	Crack 0	Crack 0'	Crack 1	Crack 2	Crack 3
64.754KN	0.5mm	0.3cm/3mm	1.2mm	2mm	3mm
%age Decrease	50%	40%	8%	20%	14%

Table A.8: Crack Width After Unloading of Beam G2B-10

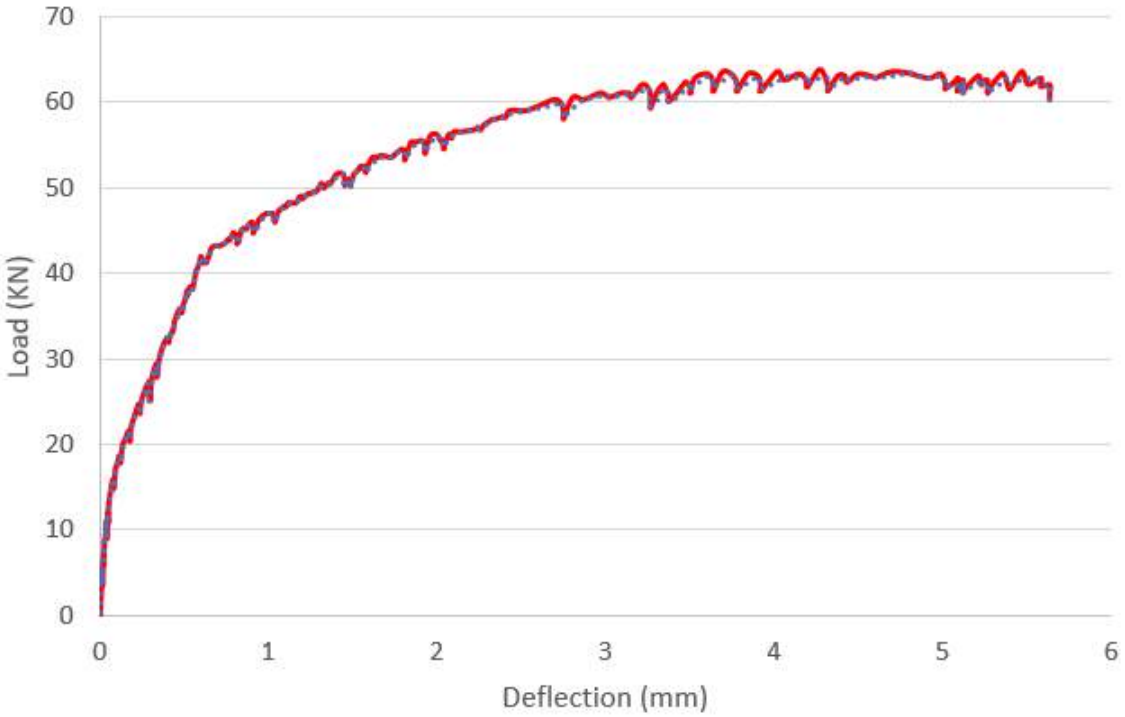

Figure A.3: Filtered Load Vs Deflection of G2B-10

Figure A.4: G2B-10 After Failure

A.4.1.3 Beam Series 1 - Test Beam One (G2B-11)

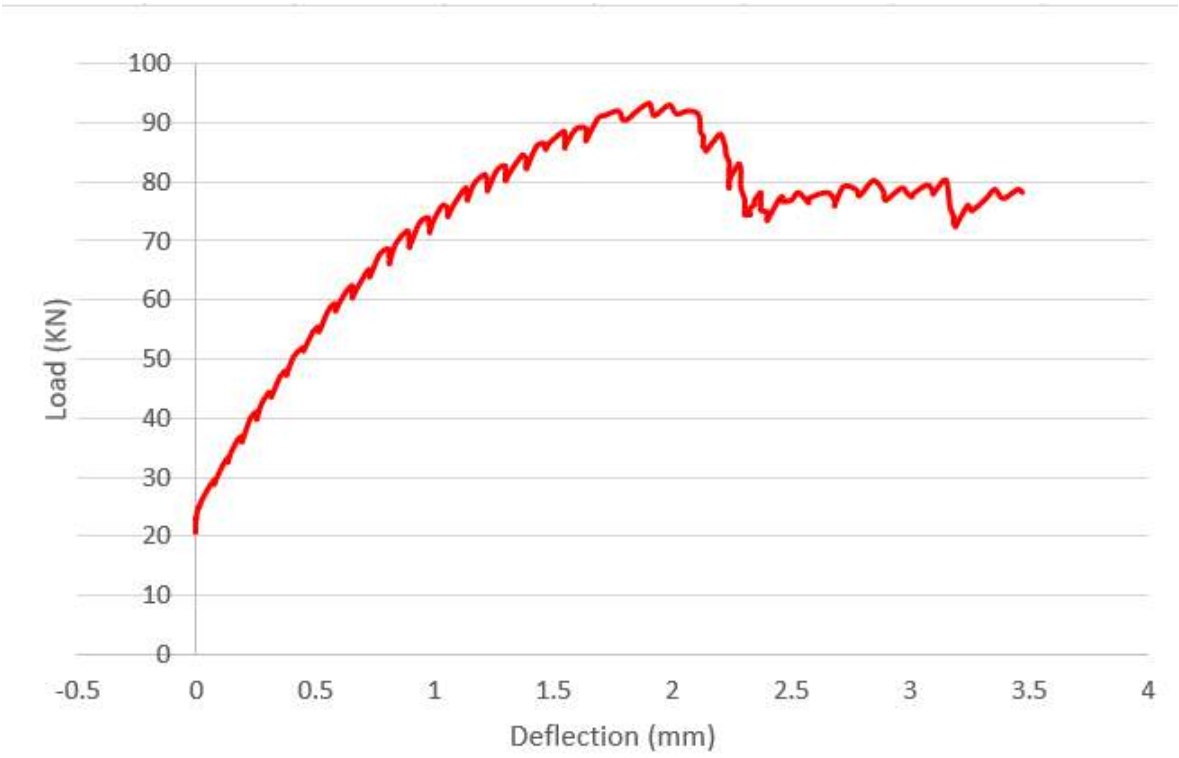

Figure A.5: Filtered Load Vs Deflection of G2B-11

Figure A.6: Concrete Crushing and Spalling at top of the beam

Delamination of G2B-11; State of delamination after failure

Figure A.7: G2B-11 After Testing Bottom, Right & Left Side CFRP Tear & Delamination (right, left & bottom)

A.4.1.4 Beam Series 1 - Test Beam Two (G2B-12)

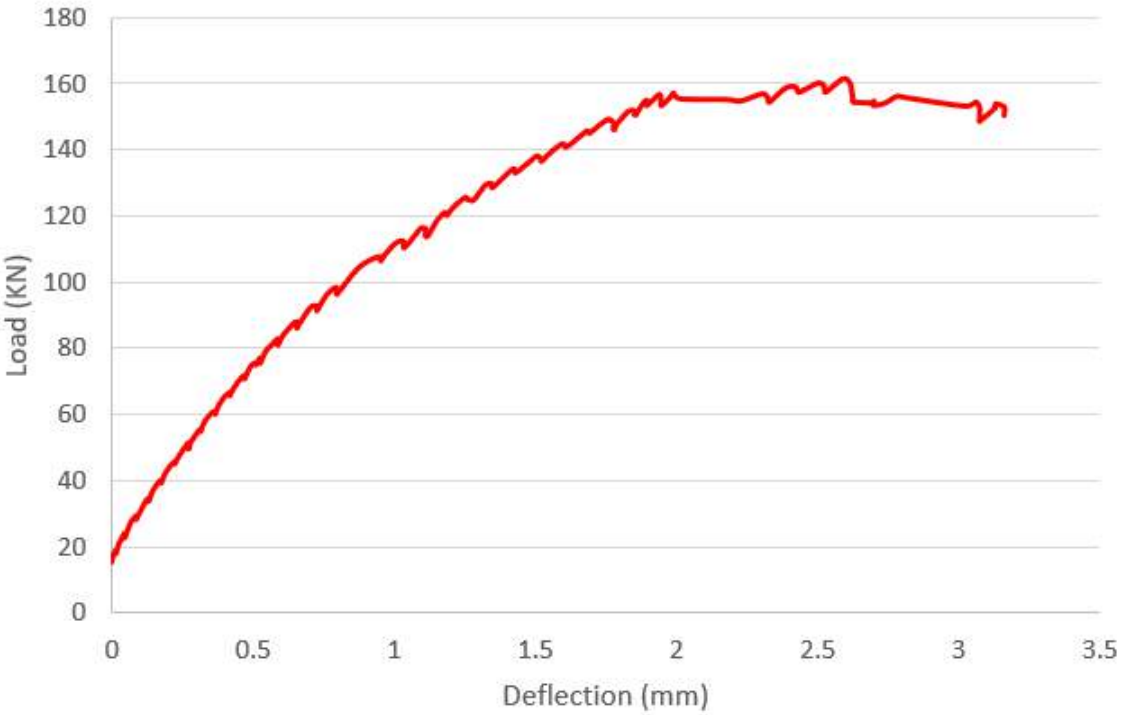

Figure A.8: Filtered Load Vs Deflection of G2B-12

Figure A.9: Concrete Crushing and Spalling at top of the beam

Figure A.10: G2B-12 Right Side CFRP Tear & Delamination

Figure A.11: G2B-12 Left Side CFRP Tear & Delamination

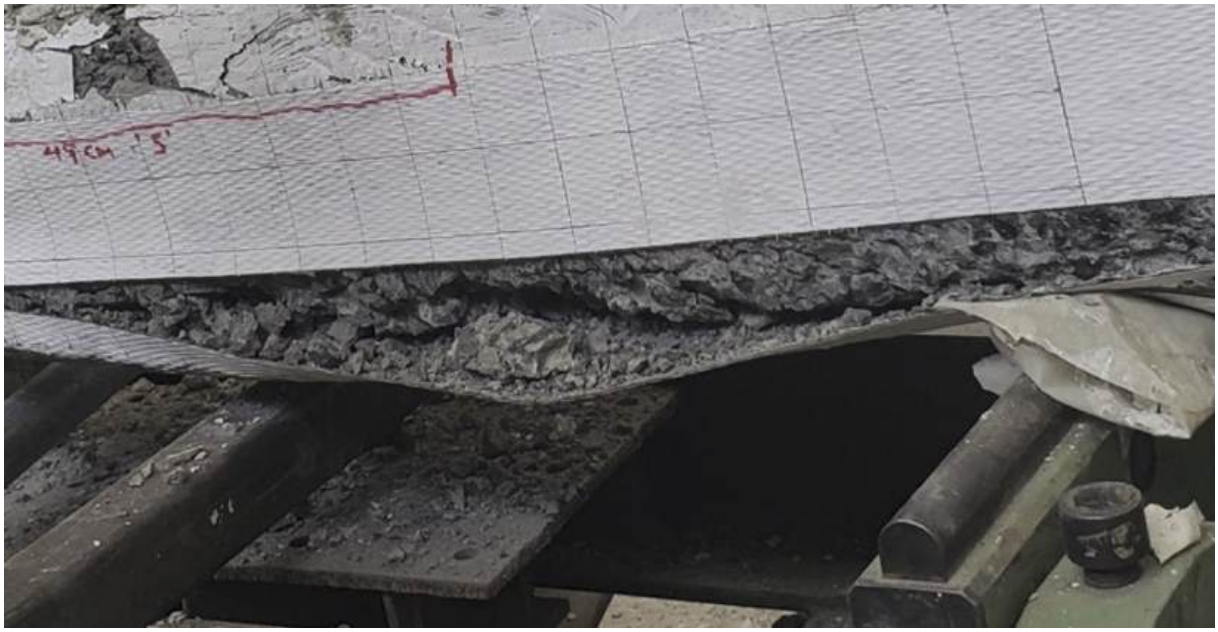

Figure A.12: Spalled Concrete Beneath the Beam G2B-12

A.4.2 Beam Series - 2

A.4.2.1 Beam Series 2 - Control Beam One (G3B-30)

Load (kN)	Crack Width (Right Side)							
	Crack 0	Crack 1	Crack 2			Crack 3		Crack 4
			2	2'	2"	3	3'	
19	0.08mm							
30	0.4mm	0.08mm						
40	0.45mm	0.7mm	0.1mm	0.04mm	0.2mm			
50	0.65mm	0.6mm	0.35mm	0.2mm	0.5mm			
60	1.5mm	1mm	0.6mm	0.65mm	0.6mm	0.2mm	0.1mm	
70	2mm	2mm	0.55mm	1mm	0.65mm	0.25mm	0.08mm	
80	3mm	5mm	0.35mm	1.5mm	0.65mm	0.2mm	0.04mm	
89.6	7mm	7mm	0.35mm	2mm	0.8mm	0.1mm	0.0mm	
91.11	3mm	10mm	0.25mm	2mm	1mm	0.06mm	0.0mm	0.6mm

Table A.9: G3B-30 Crack Summary

Figure A.13: Right Side Failure State of G3B-30

	Crack Width After Unloading							
	Crack 0	Crack 1	Crack 2			Crack 3		Crack 4
			2	2'	2"	3	3'	
Unloaded	6mm	5mm	0mm	0.75mm	0.35mm	0mm	0mm	0.35mm
%age Decrease	33.34%	50%	100%	62.5%	65%	-	100%	41.67%

Table A.10: G3B-30 Right Side Crack Summary After Unloading

	Crack Width (Left Side)							
	Crack A	Crack B	Crack C	Crack D	Crack E	Crack F	Crack G	Crack H
91.11KN	6mm	4mm	2mm	5mm	0.9mm	0.5mm	0.04mm	0.04mm
Unloaded	5mm	2mm	1.5mm	0.15mm	0.45mm	0.25mm	0mm	0mm
%age Decrease	16.67%	50%	25%	97%	50%	50%	100%	100%

Table A.11: G3B-30 Left Side Crack Summary

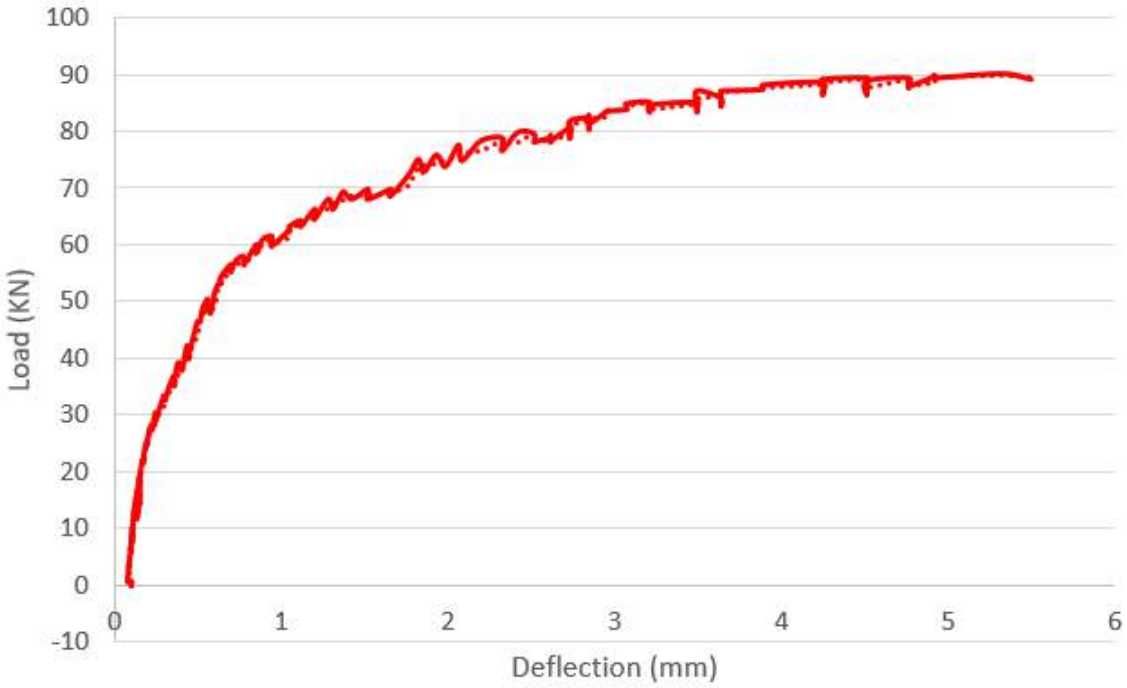

Figure A.14: Filtered Load Vs Deflection of G3B-30

Figure A.15: G3B-30 Flexural Crack and Concrete Crushing at Mid Span & at Support

A.4.2.2 Beam Series 2 - Control Beam Two (G3B-20)

Load (kN)	Crack Width (Right Side)							
	Crack 0	Crack 1		Crack 2		Crack 3	Crack 4	Crack 5
		1	1'	2	2'			
20	0.2mm							
30	0.45mm	0.2mm	0.4mm					
40	0.6mm	0.4mm	0.5mm	0.45mm	0.2mm			
50	0.8mm	0.8mm	0.6mm	0.55mm	0.45mm	0.35mm		
60	1.5mm	1.5mm	2mm	0.7mm	0.55mm	0.4mm	0.25mm	
70	5mm	3mm	2mm	1mm	0.65mm	0.55mm	0.35mm	0.3mm
73.79	12mm	5mm	3mm	1.2mm	0.45mm	0.35mm	0.3mm	0.4mm
Unloading	Invalid	3mm	1.3mm	0.45mm	0mm	0.1mm	0.04mm	0.25mm
%age Decrease	-	40%	56.67%	62.5%	100%	71.43%	86.67%	37.5%

Table A.12: G3B-20 Crack Summary

	Crack Width (Left Side)					
	Crack A	Crack A'	Crack B	Crack C	Crack D	Crack E
73.79KN	5mm	3mm	2mm	15mm	0.5mm	0.35mm
Unloaded	5mm	3mm	1.5mm	0.9mm	0.4mm	0.3mm
%age Decrease	76%	53.33%	25%	94%	20%	14.29%

Table A.13: G3B-20 Left Side Crack Summary After Unloading

.

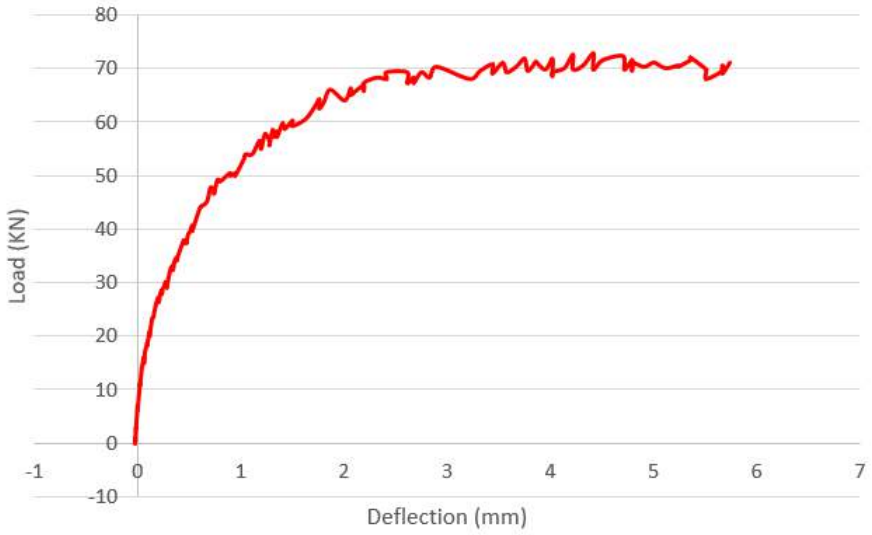

Figure A.16: Filtered Load Vs Deflection of G3B-20

Figure A.17: G3B-20 Flexural Crack and Concrete Crushing (Top & Bottom Center)

A.4.2.3 Beam Series 2 - Test Beam One (G3B-21)

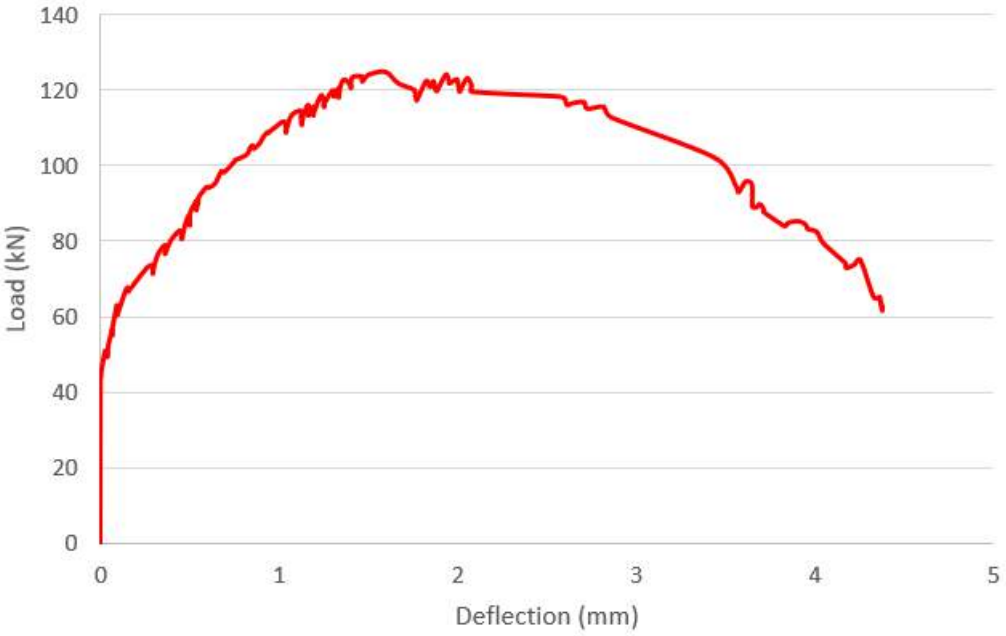

Figure A.18: Filtered Load Vs Deflection of G3B-21

Figure A.19: G3B-21 After Failure

Figure A.20: G3B-21 Right Side Tear & Delamination

Figure A.21: G3B-21 Left Side Tear & Delamination

A.4.2.4 Beam Series 2 - Test Beam Two (G3B-22)

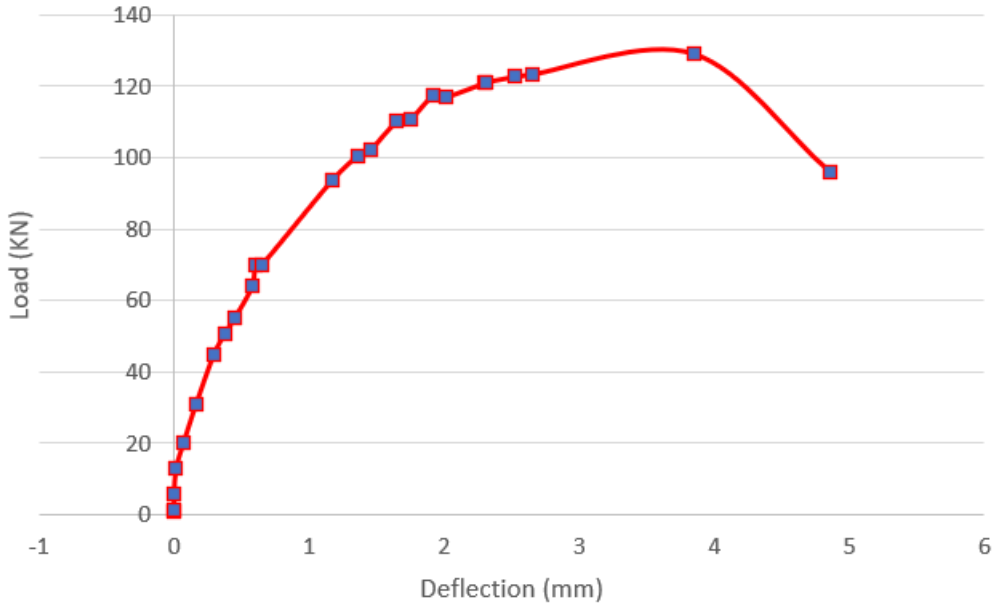

Figure A.22: Load Vs Deflection of G3B-22

Figure A.23: Concrete Crushing and Spalling at Bottom of the Beam G3B-22

Figure A.24: G3B-22 Right Side Tear & Delamination

Figure A.25: G3B-22 Left Side Tear & Delamination